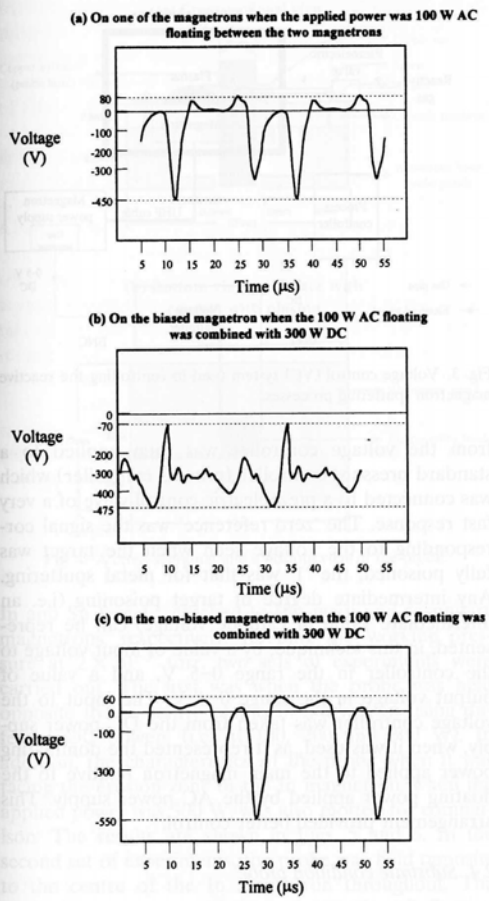

Fig. 2. A reproduction of the photographs taken from the oscilloscope for the DC potentials, relative to earth, developed on a floating, biased and non-biased Al magnetron.

was 100 W AC floating between the two magnetrons (Fig. 2a).

2. On both the biased (Fig. 2b) and the non-biased (Fig. 2c) magnetrons, when the 100-W AC floating was combined with a 300-W DC power to bias one of the magnetrons (a common case).

A similarity can be noticed between Fig. 2a,c. To understand the reason behind that, the reader is referred to Fig. 1. The capacitor shown in the AC part of the circuitry is an internal component of the output stage of the AC power supply. Its purpose is to block any DC component of current should there be any, emanating from the AC power supply, and has twofold ramifications. The first is that the current, in the AC part of the circuit, is to be the same in both directions when a DC bias is applied. Secondly, without a DC bias, the capacitor is charged/discharged following the voltage waveform of the AC power supply. Alternatively, when a DC bias is applied to one of the magnetrons, the capacitor is charged/discharged (via the biased magnetron) following the voltage difference $V_a - V_b$, where V_a is the fixed DC voltage and V_b is the alternating AC one. This leads to a slight change in the AC current in the AC part of the circuit from that when only the AC power was applied. As a result, a slight change in the voltage of the non-biased magnetron should also occur to maintain AC current magnitude in both directions. In other words, for periods when the AC current flow is in the same direction to the DC current, the capacitor will charge due to the latter. This accumulated charge is discharged onto the biased magnetron. In order to maintain AC current magnitude in both directions, the non-biased magnetron must develop an appropriate bias, as can be noticed by comparing the positive voltage regions of Fig. 2a,c. Consequently, Fig. 2a can be regarded as a representative voltage waveform for such a circuit. Comparing Fig. 2a,c, it is suggested that the AC current (in the AC part of the circuit) is indeed approximately equal in both cases. The magnitudes in both directions are approximately equal, within the biased magnetron arrangement.

On the other hand, whenever the DC potential of the magnetron is negative with respect to the plasma potential (earth potential in this case), sputtering will occur. It is easy to see, then, from Fig. 2b, that the biased magnetron is sputtering continuously, albeit to various degrees. Fig. 2c shows that the non-biased cathode is not sputtering continuously; although it attains a potential of approximately -550 V, these periods are short compared to the 'off times', when its potential goes positive with respect to plasma potential. In summary, we have:

1. The biased magnetron is tied to DC potential. The current to it is the sum of the DC current driven from the DC power supply and the current that is driven from the AC power supply. The existence of a DC bias means that the plasma has to be earthed, by contact with the chamber walls, to allow the DC current to flow.
2. The non-biased magnetron will adjust its internal DC voltage so as the AC current flowing around the AC part of the arrangement is equal in magnitude for both current directions (i.e. to both magnetrons). This results in a constant AC power applied to each cathode, provided the target materials are identical.

2.2. Plasma emission monitoring (PEM)

This method of control has been described in detail in a previous paper [6]. In the course of this work, the plasma contained mainly the emission lines corresponding to argon, oxygen and the target material. Therefore, to control the emission line/s of one of these elements, the optical filter had to be chosen so as either the wavelength/s of light it transmitted was unique to this element, or the emission intensity at the selected wavelength/s was sufficiently higher than the corresponding ones of the other two elements.

For example, for the reactive sputter-deposition of In oxide, a band pass filter had been used for controlling on In emission line at 451.1 nm. Sufficient signals up to approximately 150 mV were obtained at applied powers of the order of 300 W. At this wavelength, there is neither an argon nor an oxygen line, sufficiently intense, to interfere with the In one. A more universal technique was required for the large number of materials investigated in this work. A high-pass filter, with a cut-off wavelength at approximately 620 nm, was successfully used to control the reactive sputter-deposition of W, V, Mo and Ti oxide. At wavelengths greater than approximately 620 nm, the intensities of the emission lines of these metals are very weak. Thus, the transmitted signal by this filter is either due to argon or oxygen-lines. The signal fell as oxygen was admitted and it is concluded that the strong signal was due to argon, and the control was carried out on the argon lines, the fall in intensity being attributed to changes in the discharge current and coupling to the components of the atmosphere as the oxygen was added. Signals up to approximately 1.5–2 V were obtained at applied powers of the order of 300 W.

2.3. Voltage control

Voltage control has been described in detail in a previous paper [6]. This method of control has been used in this work in the cases of Al, Zn, Cu and Pb when they were sputtered in an Ar/O_2 atmosphere.

Fig. 3 shows a schematic of the voltage control loop. A user connector, located on the rear panel of the Advanced Energy™ power supplies which was used in this work, provides a 0–5-V DC analogue signal representing the cathode voltage (i.e. the output voltage of the power supply). The DC signal was 0 V when the output voltage of the supply was also 0 V and it was 5 V at the full-scale output voltage of the supply. This 0–5-V DC signal was used as an input to a voltage controller. The signal was taken through two controls; one of which backs it off against another potential to provide a zero reference. The difference from this zero signal was then amplified by a variable gain amplifier to give an output ranged from 0 to 1 V. The output signal

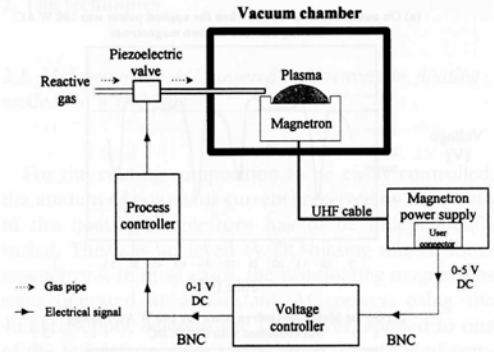

Fig. 3. Voltage control (VC) system used in controlling the reactive magnetron sputtering processes.

from the voltage controller was then applied to a standard pressure controller (process controller) which was connected to a piezoelectric control valve of a very fast response. The 'zero reference' was the signal corresponding to the voltage seen when the target was fully poisoned, the '1' was that for metal sputtering. Any intermediate degree of target poisoning (i.e. an intermediate value of cathode voltage) can be represented, in this technique, by a value of input voltage to the controller in the range 0–5 V, and a value of output voltage in the range 0–1 V. The input to the voltage controller was taken from the DC power supply, when it was used, as it represented the dominating power applied to the main magnetron relative to the floating power applied by the AC power supply. This arrangement provided better control.

2.4. Substrate condition probe

The information that was required was the ion current density to the substrate and its floating potential. In other words, the number and energy of ions that bombarded the growing films relative to the number of atoms deposited. To obtain this information, we used what we termed a 'substrate condition probe'. Fig. 4 shows a cross-sectional and a bottom view (i.e. the surface with a direct contact with the plasma) of this probe. It essentially consisted of a central cylindrical head, whose diameter was 6 mm, surrounded by a 25×37 mm guard. The guard, which was entirely isolated from the head, was utilised to minimise the plasma edge-effect from the probe head. The probe was placed in the plane of the substrate following the same procedure of placing a substrate; it was mounted in the jig, which was in turn inserted into the platen.

The I–V characteristics were then obtained by biasing the probe head. The current to the guard was excluded. Probe measurements were performed using

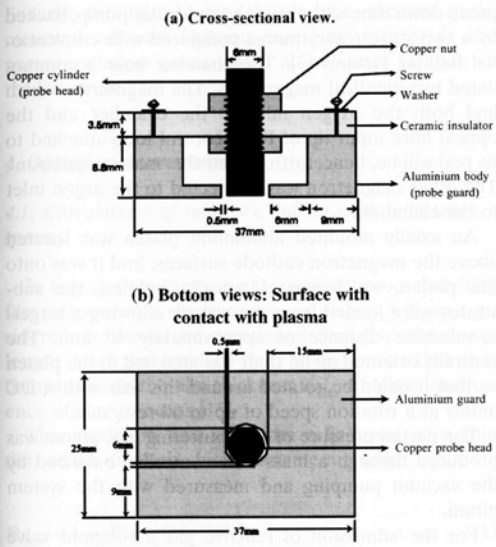

Fig. 4. A cross-sectional and a bottom view of the probe.

In and Sn targets attached to the main and secondary magnetrons, respectively. Keeping the working pressure at 2×10^{-3} torr, two sets of experiments were carried out. The first was when the probe was held opposite to the centre of the In magnetron using different DC powers (i.e. at 100, 200 and 300 W). In addition, the characteristics of the probe when it was facing the erosion zone of the In magnetron, when the applied power was 300 W, was also plotted for comparison. The results are shown in Figs. 5 and 6. In the second set of experiments, the probe was held opposite to the centre of the In magnetron throughout. The applied powers were 50 W and 100 W AC floating between the two magnetrons, and 300 W DC combined with 100 W AC. The results are shown in Fig. 7. The following remarks can be deduced from these figures:

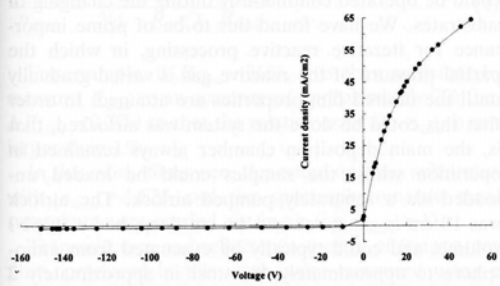

Fig. 5. The I–V characteristics of the probe when an In magnetron was held at 300 W DC and the probe was held opposite to the centre of the magnetron.

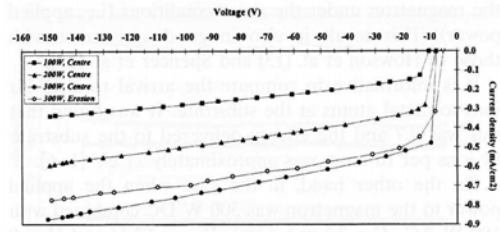

Fig. 6. The negative part of the I–V characteristics of the probe, at different DC powers to an In magnetron, when it was held opposite the centre of the magnetron. The curve when the probe was held opposite the erosion zone is also plotted.

1. The ion-current to the probe increased with the applied DC power to the magnetron. On the other hand, at a fixed DC power (e.g. 300 W), such a current was higher when the probe was held opposite the centre of the magnetron than when it was opposite the erosion zone. Similarly, the ion-current to the probe also increased with the applied floating AC power.
2. At a fixed magnitude of power (e.g. 100 W), the ion-current to the probe was lower in the DC case than in the floating AC one. Furthermore, the ion-current to the probe in the case of the 100-W AC combined with 300-W DC was the highest (Fig. 7).
3. The floating potential of the probe was almost independent of the applied AC power and slightly dependent on the DC power. However, the order of magnitude of these floating potentials was slightly lower when DC powers were applied.

The above conclusions are in very good agreement with the results obtained by Window and Savvides [12] and the results of Glocker [8]. In addition, the ion-current and floating potential, when the probe was opposite to the erosion zone, are less than the corresponding values when the probe was opposite to the centre of

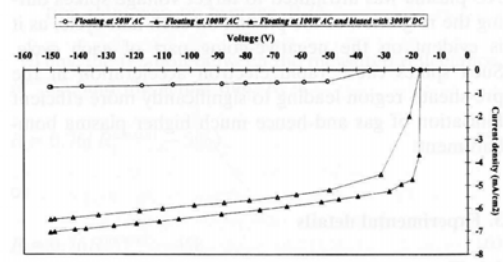

Fig. 7. The negative part of the I–V characteristics of the probe at different AC powers to a non-biased and biased floating In magnetron when the probe was held opposite the centre of the magnetron.

the magnetron under the same conditions (i.e. applied power). This result is also in good agreement with those of Howson et al. [13] and Spencer et al. [14].

It is informative to compute the arrival ratio of Ar ions to metal atoms at the substrate. It was found that this was 0.7 and the energy delivered to the substrate by ions per In atom was approximately 21 eV [1–6].

On the other hand, in the case when the applied power to the magnetron was 300 W DC combined with 100 W AC, $J_i^s = 7.1$ mA/cm^2, $V_f = -17$ V and $V_p = 0$ V (Fig. 7), where J_i^s, V_f and V_p are the ion current density to the substrate, the floating potential of the substrate and the plasma potential, respectively. Considering the case of indium oxide, which had a thickness of 152 nm, it was found that $N_i^s/N_m^s = 5.7$, where N_i^s and N_m^s are the number of ions bombarding 1 cm^2 of the substrate per second and the number of deposited metal atoms on 1 cm^2 of the substrate per second, respectively. Consequently, the energy delivered to the substrate by ions per In atom was approximately 100 eV.

Although the two magnetrons were unbalanced in the system used in this work, the measured floating potentials of the substrate were relatively low, whereas, the measured ion current densities were moderate. This could be due to the fact that target-to-substrate distance is less than the null-point of the magnetrons, which means that, at such low distance, ions cannot acquire high kinetic energies when they impinge on the substrate, with the lower floating potential that the substrates have. The small target-to-substrate distance also affects, but less severely, the ion current density, as the substrate can not collect all ions available because it is not in the way of the focused beam leaking from the cathode, rather it is in the base of that beam. The average ion densities in the AC plasma are approximately four times that of the DC plasma. This last difference, between the AC and the DC plasmas is significant. According to optical emission measurements, the plasma extinguishes on each half-cycle and has to be reignited. The increase in ion densities in the AC plasma was attributed to target voltage spikes during the reignition of the plasma on each half-cycle, as it is evident on the negative-going part of each cycle. Such spikes cause rapid electron acceleration in the pre-sheath region leading to significantly more efficient ionisation of gas and hence much higher plasma bombardment.

3. Experimental details

3.1. The sputtering system

The chamber comprised a 42-cm diameter stainless steel chamber, 12-cm deep internally, giving a short pump down time with the turbomolecular pump, backed by a two-stage rotary pump, compared with conventional bell-jar systems [3]. The chamber base accommodated two identical magnetrons. The magnetron, which had both the oxygen inlet to the chamber and the optical fibre input tip of PEM control loop attached to its pod will be, henceforth, called the 'main magnetron'. The other magnetron was connected to the argon inlet to the chamber.

An axially mounted aluminium platen was located above the magnetron cathode surfaces, and it was onto this platen, which was electrically isolated, the substrates were loaded from the airlock allowing a target-to-substrate distance of approximately 40 mm. The centrally oriented metal shaft was attached to the platen so that it could be rotated around this axis with a DC motor at a rotation speed of up to 60 rev./min.

The partial pressure of the sputtering gas, argon, was produced through a mass flow controller balanced by the vacuum pumping and measured with the system pirani.

For the admission of reactive gas a solenoid valve was replaced by a piezoelectric valve, having a faster response in order to cope with much faster changes in the desired supply of reactive gas required to maintain a certain cathode status, compared with that of inert gas. This was controlled to produce a pre-determined optical emission signal or cathode potential in much the same way as is used to control pressure. In addition, the total distance between the reactive gas pipe exit in the chamber and the piezoelectric valve was minimised to help reducing the time constant of the pipe. These modifications, allied with the pipe outlet being very close to the target in the very confined volume provided by the gettering enabled very efficient control of the reactive deposition processes to be obtained.

3.2. The airlock system

The system was designed so that the magnetrons could be operated continuously during the changing of substrates. We have found this to be of prime importance for iterative reactive processing, in which the partial pressure of the reactive gas is varied gradually until the desired film properties are attained. In order that this could be done the system was airlocked, that is, the main deposition chamber always remained in operation whilst the samples could be loaded/unloaded via a separately pumped airlock. The airlock was 10 cm in diameter and 4.6 cm deep, had a 0.361 l volume, and could typically be evacuated from atmosphere to approximately 40 mtorr in approximately 2 min, via two-stage rotary pump.

Samples were mounted singly in a jig, which was then attached to the end of a loading arm, which was moved

linearly through double Wilson-type vacuum seals, mounted off axis (2.2 cm from the centre) in the perspex window plate, which allow visual location of the substrate.

4. Optical measurements

4.1. Calculations of refractive indices from reflectance spectra

In this section, the case of transparent non-absorbing films deposited on transparent substrates will be considered. It should be mentioned first that the wavelength λ of the incident light is chosen so that it is comparable to the film thickness d_{film} to allow interference effects to occur [15].

The maximum and minimum reflectance of a thin film on an infinitely thick substrate are given by:

$$R_{\max} = \left(\frac{n_{\text{film}}^2 - n_{\text{amb}} n_{\text{subs}}}{n_{\text{film}}^2 + n_{\text{amb}} n_{\text{subs}}} \right)^2 \quad (1)$$

$$R_{\min} = \left(\frac{n_{\text{subs}} - n_{\text{amb}}}{n_{\text{subs}} + n_{\text{amb}}} \right)^2 \quad (2)$$

where $R_{\max}$, $R_{\min}$, n_{film}, n_{subs} and n_{amb} are a reflectance maximum, reflectance minimum, the refractive index of the thin film, the refractive index of the substrate and the refractive index of the ambient medium, respectively. By solving Eq. (1) for n_{film}, we get:

$$n_{\text{film}} = \left(n_{\text{amb}} n_{\text{subs}} \frac{1 + \sqrt{R_{\max}}}{1 - \sqrt{R_{\max}}} \right)^{1/2} \quad (3)$$

The relative precision of n_{film} is given by

$$\frac{\Delta n_{\text{film}}}{n_{\text{film}}} = \frac{\sqrt{R_{\max}}}{2(1 - R_{\max})} \frac{\Delta R_{\max}}{R_{\max}} \quad (4)$$

For example, if $R_{\max} = 36\%$, it is then sufficient to measure $R_{\max}$ to an accuracy of approximately 2% (i.e. $\Delta R_{\max} = 0.7\%$) so that the relative error for n_{film} is not larger than 1%.

In this work, films were deposited on glass substrates with $n_{\text{subs}} = 1.525$ and the spectrophotometric measurements were carried out in air (i.e. $n_{\text{amb}} = 1$).

Transmittance and reflectance spectra of transparent films, produced in this work, were measured using a Hitachi U-2000 double-beam spectrophotometer with a simple reflection attachment, which allowed comparison of the sample with freshly prepared aluminium

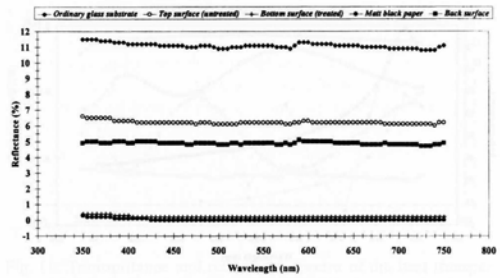

Fig. 8. Reference spectra of uncoated glass substrates in different cases. The reflectance spectrum of matt black paper is included for comparison.

coating. In spectrophotometric measurements carried out in this work, both transmittance and reflectance spectra were measured in the spectral range 350–750 nm with a scanning speed of 400 nm/min.

In order to obtain values for the absolute reflection coefficients that were required, it was necessary to make corrections of the measured reflectance spectra of the deposited films. The corrections involved:

1. Measuring the reflectance spectrum of the bottom surface of an uncoated glass substrate in order to subtract it from the measured values of reflectance. This was achieved by treating the bottom surface of an uncoated glass substrate with emery paper so virtually eliminating reflection from it (Fig. 8). The reflectance spectra of the untreated (or top) surface and that of an ordinary glass substrate were then measured. The reflectance spectrum of the back surface was obtained by subtracting the reflectance values of the top surface from those of the ordinary substrate, and was averaged to be 5%.
2. Measuring the reflectance spectrum of a single crystal silicon wafer and comparing it with a calculated one [16] to derive a correction curve of the measured reflectance in order to obtain the absolute reflectance of the coatings (Fig. 9). The correction ratio was, on average, 0.76.

Thus, the relation between the measured reflectance, R^{measur}, and the actual one, R, is

$$R \approx 0.76(R^{\text{measur}} - 5\%) \quad (5)$$

or

$$R \approx 0.76 R^{\text{measur}} - 4\% \quad (6)$$

As a result, if $R_{\max}^{\text{measur}}$ is the measured value of a reflectance maximum, the corresponding actual value, $R_{\max}$, is given by

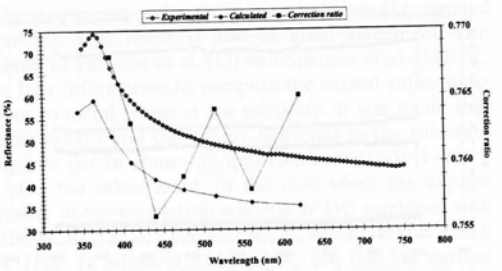

Fig. 9. Calculated and experimental reflectance spectra of a single crystal silicon wafer. Also shown is the correction ratio as a function of wavelength. Data of the calculated curve are from [16].

$$R_{\max} \approx 0.76 R_{\max}^{\text{measur}} - 4\% \tag{7}$$

Thus, by substituting the value of $R_{\max}$:

$$n_{\text{film}} = \left(1.525 \frac{1 + \sqrt{0.76 R_{\max}^{\text{measur}} - 0.04}}{1 - \sqrt{0.76 R_{\max}^{\text{measur}} - 0.04}} \right)^{1/2} \tag{8}$$

Instead of ellipsometry, Eq. (8) was used to calculate refractive indices of films produced in the course of this work, for the following reasons:

1. It is independent of optical thickness of coatings and consequently gives consistent results for variable optical thickness.
2. The possibility of obtaining refractive indices over many wavelengths rather than at 632.8 nm using the ellipsometer that was available.
3. The ratio of the area of light beam of the spectrophotometer (~ 10.8 mm^2) and that of the laser beam of the ellipsometer (~ 0.8 mm^2) is approximately 14. This gives better integration over the coated area of the substrate.

4.2. Calculations of thickness from reflectance spectra using interference methods

After calculating n_{film}, using Eq. (8) the film thickness could be calculated using equations $n_{\text{film}} d_{\text{film}} = (2k+1)\frac{\lambda_{\max}}{4}$ and $n_{\text{film}} d_{\text{film}} = k\frac{\lambda_{\min}}{2}$, where $\lambda_{\max}$ is a wavelength at which a reflectance maximum occurs and $\lambda_{\min}$ is a wavelength at which a reflectance minimum occurs. The calculation procedure depended on the shape of the reflectance spectrum of interest.

If there were two consecutive maxima in the scanned spectral range, then for the first maximum $4 n_{\text{film}} d_{\text{film}} = (2k+1)\lambda_{\max_1}$ and that for the second maximum is $4 n_{\text{film}} d_{\text{film}} = [2(k-1)+1]\lambda_{\max_2}$. By solving these two equations, it is found that

$$d_{\text{film}} = \left| \frac{\lambda_{\max_1} \lambda_{\max_2}}{2 n_{\text{film}} (\lambda_{\max_2} - \lambda_{\max_1})} \right| \tag{9}$$

Eq. (9) is also valid in the case of two consecutive minima. The problem of this equation is that it ignores changes of n_{film} with wavelength. However, it was considered to be sufficiently accurate for the estimation of d_{film} for the purpose of this work, especially in the relatively narrow range of wavelength studied where variations in n_{film} were not expected to be so significant.

Finally, it should be indicated that the results of the thickness measurements were satisfactorily consistent in the course of this work.

5. Results

5.1. Aluminium oxides

The system was established using aluminium cathodes in both magnetrons. Aluminium oxide is a very insulating oxide with a high secondary electron emission coefficient, which leads to extreme arcing if DC reactive sputtering is attempted.

In this work, Al_2O_3 films were prepared using the mid-frequency AC powered magnetrons technique. The main and secondary targets were both Al and the two magnetrons were operated in the floating mode at $P^{\text{AC}}_{\text{Al}\leftrightarrow\text{Al}} = 1$ kW. Substrates were held static over the main magnetron. In this case, no incorporation of an alloying material was required. Voltage control on the main Al magnetron was used. The percentage of aluminium magnetron voltage set point, $\text{Al}^{\%}_{\text{vc}}$, was gradually decreased and a film was deposited and characterised at each value of $\text{Al}^{\%}_{\text{vc}}$. The deposition time was 3 min. Fig. 10 shows the dependence of transmittance at 550 nm, T_{550}, of the visibly transparent Al_2O_3 films, and the corresponding deposition rate, on $\text{Al}^{\%}_{\text{vc}}$. Obviously, films of higher T_{550} are deposited at lower rates. The percentage of Al magnetron voltage set point, and the corresponding O_2 flow rate, at which the best Al_2O_3 film occurred (i.e. the one of the highest transmittance and deposition rate) were 73.7% and 3.6 sccm, respectively. The transmittance at 550 nm, refractive index and deposition rate of this film were 89.5%, 1.67 and 2.02 nm/s, respectively. Clearly, such a result is comparable with the best reported results [9,17,18], taking into account that the applied power in this work was only 1 kW. Fig. 11 shows the transmittance and reflectance spectra of the best Al_2O_3 film. Finally, it is worth mentioning that, in addition to glass, aluminium oxide films have also been deposited, using this technique, on stainless steel and single crystal silicon substrates for extended periods of time (up to 45 min) and at high rates without any sign of arcing.

5.2. Mixed insulating oxides

Finally, a large number of oxide films of Mo, W, V, Pb, Ti, Sn and Cu doped with dopants such as Zn, Sn, Ti, Nb, Ta, Mo or Bi have been deposited, at different combinations of powers and at different stoichiometries, and characterised. They were initially investigated for conductivity. Although the transparent films were insulating under the deposition conditions and procedures followed (i.e. unintentional heating or biasing of substrates and no post-deposition heat treatment), their optical properties (e.g. a very wide range of refractive indices) are of great interest in optical applications.

Table 1 summarises the preparation conditions and the optical properties of some of the transparent insulating oxide films prepared in this work, where P_{Cu}^{DC}, P_{W}^{DC}, P_{V}^{DC}, P_{Mo}^{DC} and P_{Pb}^{DC} are the DC biasing powers applied to the floating Cu, W, V, Mo and Pb magnetrons, respectively, and $Cu_{vc}^{\%}$ and $Pb_{vc}^{\%}$ are the percentages of metallic Cu and Pb magnetrons voltages set-points (i.e. the occurrence), respectively. The floating AC power and deposition time were 100 W and 6 min, respectively, throughout.

6. Conclusion

According to the above discussion, the deposition technique, employed in the course of this work, enjoys the following major advantages

1. Substrate rotation enhances atomic level mixing of the film constituents. The stoichiometry of the film is controlled by PEM or voltage control, on one magnetron, and dopants are added by sputtering from the other magnetron. This means that the former magnetron serves two purposes; the first is to sputter metal and oxidise it, and the second purpose is to oxidise the metal sputtered from the other magnetron.
2. The combination of DC and mid-frequency AC power in a novel way, using a filter to protect the DC power supply from the AC one (or the independently DC powered magnetrons method), permits the composition of the produced films to be easily and independently manipulated by varying the magnitude of power applied to each magnetron. As a result, this system is able to obtain a sputter-deposited coating of an alloy or multi-element compound which is either difficult or impossible to be formed from a single target.
3. Depending on the materials involved, the use of very fast feedback methods, to automatically control the admission rate of the reactive gas (e.g. oxygen) into the sputtering chamber (i.e. PEM and voltage control), allows the stoichiometry of the deposited films to be independently controlled. The very efficient control of the admission rate of oxygen also allows the deposition rate of reactively sputtered films to be high.
4. The use of an airlocked system allows the implementation of an iterative deposition process to vary coating stoichiometry and composition. Hence, information regarding different composition and stoichiometry can be attained rapidly without cathode acquisition or preparation.
5. The system, described in this work, is superior to the dual magnetron technique described by Lewin and Howson [19] where two concentric cathode annuli of different materials (with separate magnetic fields) comprise one magnetron device in that the two sources sputter independently of each other. This permits variable compositions to be selected only to a limited extent in a reactive environment, the limit being reached when differential poisoning of the two cathode materials dominates. Clearly, precise stoichiometry control also suffers from this problem as a direct result of the close proximity of the cathode.
6. The use of mid-frequency (i.e. 40 kHz) AC power in the floating mode secures periodical effective

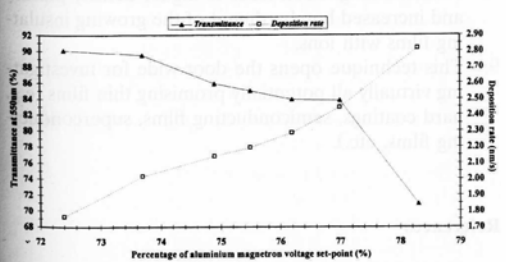

Fig. 10. Transmittance at 550 nm and the corresponding deposition rate vs. the percentage of aluminium magnetron voltage set-point of visibly transparent films of aluminium oxide. The floating AC power between the two Al magnetrons was 1 kW.

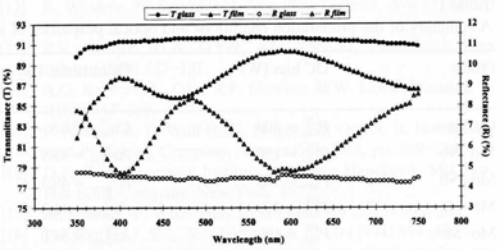

Fig. 11. Transmittance and reflectance spectra of the best transparent Al oxide film which occurred at 73.7% of Al magnetron voltage set-point. The floating AC power was 1 kW. The relevant spectra of an uncoated glass substrate are also plotted.

Table 1
A summary of the preparation conditions and optical properties of some of the transparent insulating oxide films prepared in this work[a]

Oxide	DC bias (W)	Occurrence (%)	n_{film}	T_{550} (%)	Deposition rate (nm/s)
Cu–Sn	$P^{DC}_{Cu} = 300$	$Cu^{\%}_{vc} = 30.8$	1.92	67.7	0.80
Mo–Nb	$P^{DC}_{Mo} = 150$	$Ar^{\%}_{pem} = 53.9$	2.24	72.3	0.36
Mo–Nb	$P^{DC}_{Mo} = 300$	$Ar^{\%}_{pem} = 49.3$	1.96	91.9	0.41
Mo–Nb	$P^{DC}_{Mo} = 450$	$Ar^{\%}_{pem} = 46.3$	1.93	91.9	0.44
Mo–Sn	$P^{DC}_{Mo} = 100$	$Ar^{\%}_{pem} = 54.0$	2.00	81.4	0.30
Mo–Sn	$P^{DC}_{Mo} = 300$	$Ar^{\%}_{pem} = 51.4$	2.17	90.8	0.37
Mo–Ta	$P^{DC}_{Mo} = 450$	$Ar^{\%}_{pem} = 45.9$	2.09	90.9	0.42
Pb	$P^{DC}_{Pb} = 400$	$Pb^{\%}_{vc} = 54.0$	2.46	74.2	1.25
Pb–Bi	$P^{DC}_{Pb} = 100$	$Pb^{\%}_{vc} = 52.0$	2.44	80.9	0.84
Pb–Bi	$P^{DC}_{Pb} = 300$	$Pb^{\%}_{vc} = 42.8$	2.40	88.4	1.28
Pb–Bi	$P^{DC}_{Pb} = 400$	$Pb^{\%}_{vc} = 41.4$	2.39	84.0	1.55
Ti	$P^{DC}_{Ti} = 400$	$Ar^{\%}_{pem} = 65.1$	2.63	80.1	0.05
Ti–Nb	$P^{DC}_{Ti} = 400$	$Ar^{\%}_{pem} = 69.1$	2.60	67.1	0.09
Ti–Ta	$P^{DC}_{Ti} = 400$	$Ar^{\%}_{pem} = 67.7$	2.28	69.9	0.17
V–Mo	$P^{DC}_{V} = 200$	$Ar^{\%}_{pem} = 68.9$	1.80	77.9	0.52
V–Mo	$P^{DC}_{V} = 300$	$Ar^{\%}_{pem} = 65.6$	1.79	81.4	0.48
W	$P^{DC}_{W} = 400$	$Ar^{\%}_{pem} = 51.6$	2.23	76.4	0.76
W–Mo	$P^{DC}_{W} = 150$	$Ar^{\%}_{pem} = 53.8$	2.29	91.2	0.34
W–Mo	$P^{DC}_{W} = 450$	$Ar^{\%}_{pem} = 50.0$	2.20	87.0	0.71
W–Nb	$P^{DC}_{W} = 200$	$Ar^{\%}_{pem} = 62.1$	2.29	90.8	0.38
W–Nb	$P^{DC}_{W} = 350$	$Ar^{\%}_{pem} = 51.9$	2.21	84.8	0.70
W–Nb	$P^{DC}_{W} = 400$	$Ar^{\%}_{pem} = 55.1$	2.14	74.0	1.37
W–Sn	$P^{DC}_{W} = 100$	$Ar^{\%}_{pem} = 51.9$	2.14	91.5	0.36
W–Ta	$P^{DC}_{W} = 200$	$Ar^{\%}_{pem} = 60.6$	2.29	78.1	0.59
W–Ta	$P^{DC}_{W} = 400$	$Ar^{\%}_{pem} = 56.8$	2.21	70.7	0.83
W–Ta	$P^{DC}_{W} = 600$	$Ar^{\%}_{pem} = 56.3$	2.12	86.3	1.05
W–Ti	$P^{DC}_{W} = 150$	$Ar^{\%}_{pem} = 55.6$	2.31	91.1	0.35
W–Ti	$P^{DC}_{W} = 450$	$Ar^{\%}_{pem} = 52.0$	2.24	87.9	0.64

[a]The floating AC power was 100 W throughout.

discharging of the insulating layer, due to the symmetrical operation of the electrodes. This allows the reactive sputtering process to be arc-free [9], and hence, eliminating the undesired effects of arcing in reactive sputtering such as driving the process to become unstable, creating defects in the films and reducing the target lifetime. Consequently, the defect density in insulating films is reduced by orders of magnitude [11] in comparison with the DC technique.

7. The well-defined DC conducting anode allows the sputtering process to have long-term stability, at a given set point. In addition, the high deposition rates obtained are comparable with those of the DC technique [7,9].
8. Unlike the additional complexity of the RF technique, the coupling of the AC power to the cathodes, in the frequency range used, is simple. Consequently, the AC technique can be easily adopted for sputtering from larger area cathodes [9]. On the other hand, the AC plasma used with an unbalanced magnetron leads to higher density plasma and increased bombardment of the growing insulating films with ions.
9. This technique opens the door wide for investigating virtually all potentially promising thin films (e.g. hard coatings, semiconducting films, superconducting films, etc.).

References

[1] N. Danson, I. Safi, G.W. Hall, R.P. Howson, Surf. Coat. Technol. 99 (1998) 147–160.
[2] R.P. Howson, N. Danson, I. Safi, Thin Solid Films 351 (1999) 32–36.

[3] R.P. Howson, I. Safi, G.W. Hall, N. Danson, Nucl. Instrum. Methods Phys. Res. B 121 (1997) 96–101.
[4] I. Safi, N. Danson, R.P. Howson, Surf. Coat. Technol. 99 (1998) 33–41.
[5] I. Safi, R.P. Howson, Thin Solid Films 343-44 (1999) 115–118.
[6] I. Safi, Surf. Coat. Technol. 127 (2-3) (2000) 203–219.
[7] J. Szczyrbowski, C. Braatz, SPIE 1727 (1992) 122–136.
[8] D.A. Glocker, J. Vac. Sci. Technol. A 11 (6) (1993) 2989–2993.
[9] M. Scherer, J. Schmitt, R. Latz, M. Schanz, J. Vac. Sci. Technol. A 10 (4) (1992) 1772–1776.
[10] G. Este, W.D. Westwood, J. Vac. Sci. Technol. A 6 (3) (1988) 1845–1848.
[11] S. Schiller, K. Goedicke, J. Reschke, V. Kirchhoff, S. Schneider, F. Milde, Surf. Coat. Technol. 61 (1993) 331–337.
[12] B. Window, N. Savvides, J. Vac. Sci. Technol. A 4 (3) (1986) 453–456.
[13] R.P. Howson, H.A. Ja'Fer, A.G. Spencer, Thin Solid Films 193-94 (1990) 127–137.
[14] A.G. Spencer, K. Oka, R.P. Howson, R.W. Lewin, Vacuum 38 (1988) 857–859.
[15] F. Abeles, in: E. Wolf (Ed.), Progress in Optics, II, North-Holland Publishing Company, Amsterdam, 1963, pp. 249–288.
[16] D.E. Gray, American Institute of Physics Handbook, McGraw-Hill Book Company, New York, 1972.
[17] M. Scherer, P. Wirz, Thin Solid Films 119 (1984) 203–209.
[18] P.J. Clarke, J. Vac. Sci. Technol. A 12 (2) (1994) 594–597.
[19] R.W. Lewin, R.P. Howson, Proc. 6th Int. Conf. on Ion and Plasma Assisted Techniques, Brighton, UK, (1987) pp. 464–469.

Appendix 1039-B

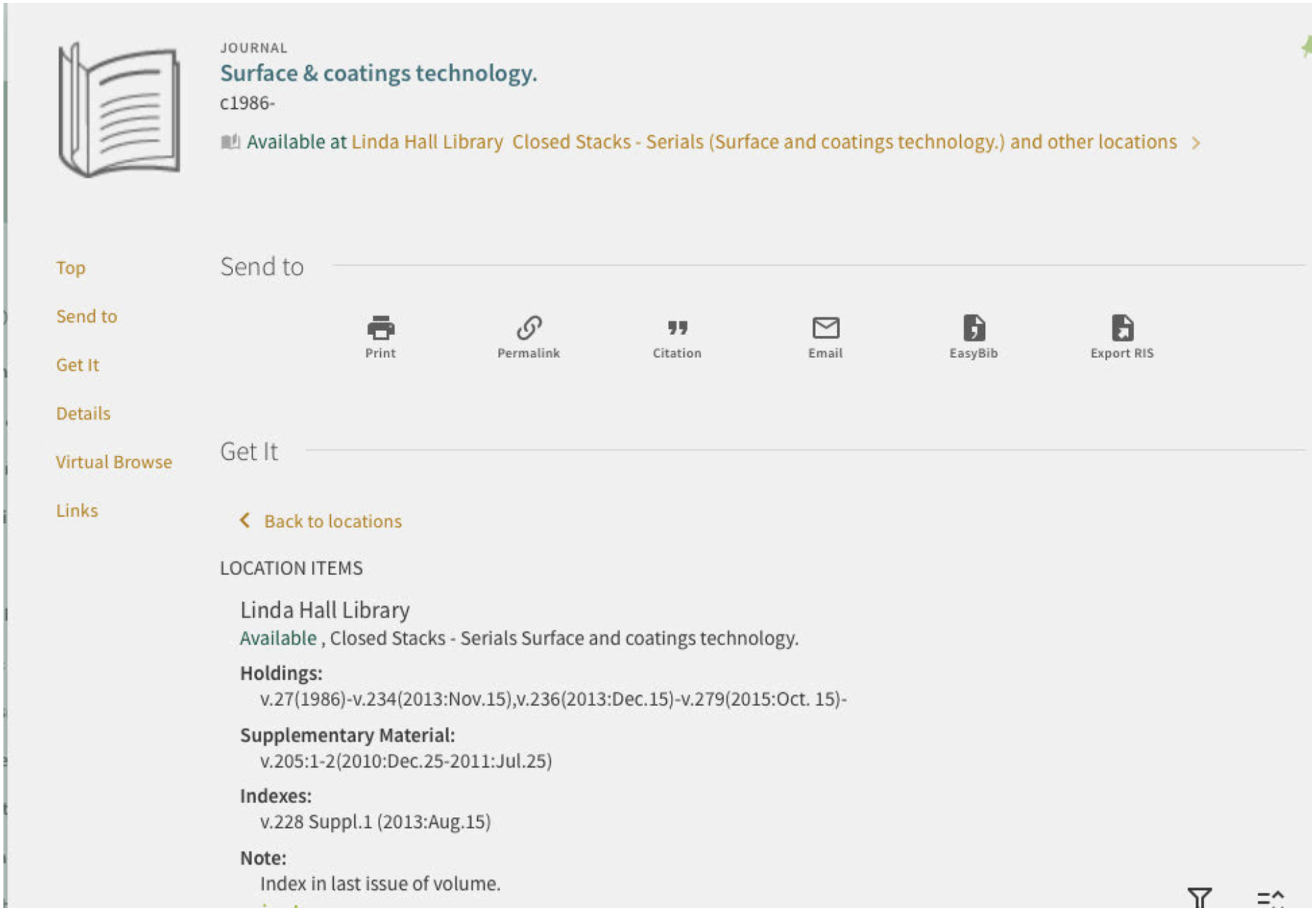
JOURNAL
Surface & coatings technology.
c1986-
Available at Linda Hall Library Closed Stacks - Serials (Surface and coatings technology.) and other locations
Top
Send to
Get It
Details
Virtual Browse
Links
Send to
Print
Permalink
Citation
Email
EasyBib
Export RIS
Get It
Back to locations
LOCATION ITEMS
Linda Hall Library
Available , Closed Stacks - Serials Surface and coatings technology.
Holdings:
v.27(1986)-v.234(2013:Nov.15),v.236(2013:Dec.15)-v.279(2015:Oct. 15)-
Supplementary Material:
v.205:1-2(2010:Dec.25-2011:Jul.25)
Indexes:
v.228 Suppl.1 (2013:Aug.15)
Note:
Index in last issue of volume.

Set It

Details

Virtual Browse

Links

Details

Title	Surface & coatings technology.
Subjects	Electroplating -- Periodicals Metals -- Finishing -- Periodicals Surface preparation -- Periodicals Coating processes -- Periodicals Surfaces (Technology) -- Periodicals
Identifier	LC : 86642343 ISSN : 0257-8972 OCLC : (OCoLC)13170399
Other title	Surf. coat. technol. Surface & coatings technology Surface and coatings technology
Related title	Earlier title : Surface technology
Publisher	Lausanne : Elsevier Sequoia Vol. 27, no. 1 (Jan. 1986)-
Creation date	c1986-
Frequency	Twelve issues a year
Citation/References note	Chemical abstracts 0009-2258 1986- Computer & control abstracts 0036-8113 1986- Electrical & electronics abstracts 0036-8105 1986- Physics abstracts 0036-8091 1986-
Local notes	Issues dated Jan.25, 2015 thru Sept. 15, 2015 still have not been received-- August 31, 2016.

```
01853cas a2200481 a 4500
993036823405961
20191030185409.0
860219c19869999sz mxzp       0   a0eng d
##$a   86642343
##$a3 $i8609 $k1 $m0
0#$a0257-8972
##$aSCTEEJ
##$a(OCoLC)13170399
##$9418209
##$a(MoKL)303682-lhalldb
##$a(lhalldb)303682-lhalldb
##$bP.0. Box 851, 1001 Lausanne 1, Switzerland
##$aLYU $cLYU $dDLC $dNSD $dDLC $dNST $dDLC $dNST $dNSD $dNST $dOCL $dHUL $dNSD
##$alc $ansdp
##$aLHLA
00$aTS670.A1 $bE43
0#$aSurf. coat. technol.
#0$aSurface & coatings technology
00$aSurface & coatings technology.
18$aSurface and coatings technology
##$aLausanne : $bElsevier Sequoia, $c[c1986-
##$aTwelve issues a year
0#$aVol. 27, no. 1 (Jan. 1986)-
2#$aChemical abstracts $x0009-2258 $b1986-
2#$aComputer & control abstracts $x0036-8113 $b1986-
2#$aElectrical & electronics abstracts $x0036-8105 $b1986-
2#$aPhysics abstracts $x0036-8091 $b1986-
##$aIssues dated Jan.25, 2015 thru Sept. 15, 2015 still have not been received-- August 31, 2016.
#0$aElectroplating $vPeriodicals.
#0$aMetals $xFinishing $vPeriodicals.
#0$aSurface preparation $vPeriodicals.
#0$aCoating processes $vPeriodicals.
#0$aSurfaces (Technology) $vPeriodicals.
00$tSurface technology $x0376-4583 $w(DLC) 76644021 $w(OCoLC)2679664
##$aArU $aCSt $aCU-A $aCU-S $aCU-SB $aCaOTU $aDLC $aIaAS $aInLP $aKyLoU $aMH-GM $aMiD $aMiU $aMnU $aMoKL $aNIC $aNN $aNNE $aNcRS $aNcU $aNjP $aPBL
##$aSurface & coatings technology.
##$cSer
##$aJan. 1986
##$aSurface and coatings technology. $bSurface & coatings technology.
##$aLTI 11/10/2017
```

Appendix 1039-C

Item Details

FMT	SE
LDR	as a2200241 a 4500
001	007514620
003	Uk
005	20100326133557.0
007	ta
008	860219c19869999sz srzp 0 a0eng d
0220	|a 0257-8972
040	|a Uk |c Uk |d Uk
08204	|a 671.7 |2 21
084	|a TJ 40 |2 blsrissc
2100	|a Surf. coat. technol.
222 0	|a Surface & coatings technology
24500	|a Surface and coatings technology.
260	|a Lavsanne : |b Elsevier Sequoia, |c 1986-
260	|a Lausanne : |b Elsevier Sequoia, |c [c1986-
300	|a v. : |b ill. ; |c 24 cm.
310	|a Semimonthly, |b <2002->
321	|a Twelve issues a year
336	|a text |2 rdacontent
337	|a unmediated |2 rdamedia
338	|a volume |2 rdacarrier
3620	|a Vol. 27, no. 1 (Jan. 1986)-
595	|a FORMERLY 8547.951 UP TO VOL. 26, 1985 SEE ALSO 8547.951 FOR SML HOLDINGS SEE ALSO CARD INDEX.
650 0	|a Electroplating |v Periodicals.
650 0	|a Metals |x Finishing |v Periodicals.
650 0	|a Surface preparation |v Periodicals.
650 0	|a Coating processes |v Periodicals.
650 0	|a Surfaces (Technology) |v Periodicals.
78000	|t Surface technology |x 0376-4583
945	|a SURFACE AND COATINGS TECHNOLOGY.
LKR	|a PAR |b 010507747 |l BLL01 |r 78000 |m Surface & coatings technology |n SURFACE TECHNOLOGY -ELSEVIER SEQUOIA-.
85241	|a British Library |b DSC |j 8547.720000

8**66 0** |a Vol. 27, no. 1 (1986)-v. 204, no. 4 (2009) |z UKRR Retained Title |z Stock Incomplete
8**527**1 |a British Library |b STI |k (P) |h TJ 40 |m -E(7) |2 blsrissc
8**66 0** |a Vol.27 (1986)-v. 135 (2001)
S**YS** 007514620

Appendix 1039-D

Arc Handling in Reactive DC Magnetron Sputter Deposition

A. Blondeel and W. De Bosscher, Bekaert Advanced Coatings (Bekaert VDS), Deinze, Belgium

Key Words: Reactive sputter deposition, Arcing, Magnetron design, Power supplies

ABSTRACT

The strong development of reactive sputter deposition is seriously hampered by instabilities that occur during these processes. One of these instabilities originates at the cathode. During the reactive DC magnetron sputter deposition of highly insulating (nitride and oxide) films from metallic targets, an electrically insulating layer is not only formed on the substrate but also on the target (cathode) surface, leading to charge build-up and consequently to arcing. These arcing events are detrimental for the deposition process itself and for the deposited thin film.

The use of rotating targets already drastically reduces the probability of arcing compared to planar targets: for a rotatable target, arcing only occurs at the target tube ends. In this paper, additional arc preventing hardware enhancements for rotating targets are proposed, as well as improved arc-handling electronics. Firstly, a special treatment of the target tube ends is examined (application of a dielectric anti-arcing layer). Secondly, a more flexible and more practical alternative consists of the addition of a target tube end anti-arcing guard ring (a ring shaped part of the target clamping system). Finally, an in-house developed power supply and arc suppressor, both based on the same advanced electronics, are presented. These enhancements provide us with drastically increased process stability.

INTRODUCTION

The need to deposit high quality dielectric films at high rate is gaining ever more importance. These dielectric films (such as Al_2O_3 and SiO_2) are deposited using reactive sputtering from conductive targets by the introduction of a reactive gas (e.g. oxygen) next to the inert gas (e.g. argon) used in the conventional sputtering process. Several intrinsic problems are associated with reactive sputter deposition (e.g. hysteresis phenomena, poor deposition rate due to target poisoning, inhomogeneities, disappearing anode related phenomena and arcing) and special precautions are necessary to anticipate these problems when performing reactive sputter deposition on industrial scale [1–3]. One of the problems, originating at the cathode surface, is arcing. As the coating process proceeds, not only the substrate and the chamber walls but also the cathode surface and especially the areas next to the racetrack are covered with an insulating layer. This insulating layer charges up by ionic bombardment and when the dielectric strength is exceeded, electrical breakdown occurs, leading to arc discharges. The arc discharges are detrimental for the deposition process itself, for the deposited thin film and even for the sputter equipment. Arc discharges can drive the process to become instable, inhomogeneities and defects are created in the growing film, target lifetime is reduced by liquid droplet ejection (causing new arc events originating at the damaged areas) and the power supply can be harmed. Because of these problems arcing is the subject of a lot of research [4–8]. The introduction of large size rotating cylindrical targets has restricted the arcing zone to two ring shaped areas at the cathode tube ends (next to other benefits offered by cylindrical cathodes such as higher target utilization, higher power densities and more compact size). Compared to similar planar targets the arcing probability is reduced to less than 5%. This is illustrated in Figure 1.

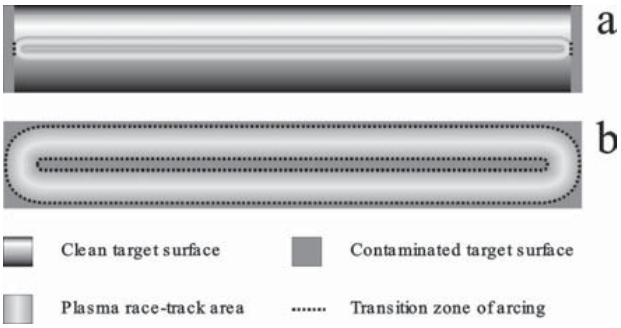

Figure 1. Schematic view of target surface conditions and arcing zone for (a) rotating cylindrical and (b) planar magnetron.

Little arcing occurs in the racetrack area of rotating cylindrical targets since it is continuously cleaned by the plasma. The latter is only true on condition that target rotation speed is high enough, otherwise the target surface in the racetrack area is contaminated before it is sputter cleaned leading to arc events. Typically, a rotation speed of 10 rpm is sufficient. Moreover, the arc sensible zone for rotating cylindrical targets is independent of the target length. Despite this drastic improvement, arc management is still needed during reactive DC magnetron sputtering. The present paper focuses on the

44th Annual Technical Conference Proceedings—Philadelphia, April 21–26, 2001 ISSN 0737-5921

prevention of arcing by removing the cause (hardware enhancements) and on an improved way of handling eventual arc events (detection and suppression) electronically.

EXPERIMENT DETAILS

The research was performed in a semi-industrial test chamber (illustrated in Figure 2) containing one rotating cylindrical Al target with a length of about 1 m and one (screened) Cyclomag® (not used in this research). The DC power was applied to the cathode using an in-house developed 100 kW power supply. The experiments were done typically at 20 to 25 kW, both in constant current and constant power mode. Arcing was evaluated by visual inspection of the target tube ends and by counting the arc events using an in-house developed arc suppressing unit. Each experiment was started by metallic sputtering of Al in Ar atmosphere (sputter cleaning of the target) in the pressure range of 1 to 2 10^{-3} mbar, using an Ar flow of 50 to 60 sccm. This was continued until the process was stable and the occurrence of arcing was only exceptional. The reactive sputtering in an Ar/O_2 mixture was started by setting the Al signal of the PEM04 control unit (Von Ardenne) to 30% of its initial value in metallic mode, corresponding with an O_2 flow of approximately 70 sccm. Arc counting was started immediately. In this way the arcs were counted during a sputter process corresponding with a condition on the edge of the hysteresis slope from metallic to poisoned sputtering. In order to evaluate the arc preventing hardware enhancements in an optimal way, all (major and minor) arcs were taken into account (sensitive setting of the arc suppressing unit). The experiment was ended by shutting down the power supply.

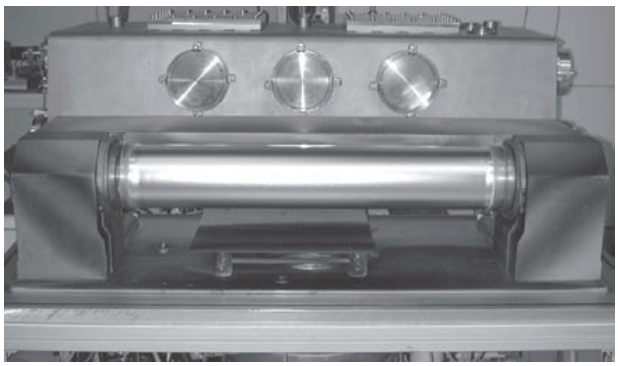

Figure 2. Semi-industrial test chamber for applied research on plasma instabilities.

In a first series of experiments, the prevention of arcing during reactive DC sputtering is examined. This is done by preventing the redeposited oxide layer of reaching electrical breakdown. A protective arc-inhibiting dielectric layer is applied on the arc sensitive areas. Different dielectric layers (different materials, applied in a variety of ways) were tested and submitted to semi-industrial sputter conditions. During the research it was found that the exact positioning of the dielectric anti-arcing layers was extremely important, so a lot of effort was put in the optimization of the dielectric layer width.

Since the application of this protective layer is rather unpractical for real industrial environment, a more flexible and more practical alternative is proposed, consisting of the addition of an adjustable dielectric target tube end anti-arcing guard ring.

During the second series of experiments the arc handling capabilities of in-house developed sputter electronics was tested. These in-house developed sputter electronics consist of a compact 2*100 kW DC power supply, an arc suppressing unit and a low frequency (below 1 kHz) switching unit. The last two components were also evaluated in combination with other commercially available DC power supplies.

ARC PREVENTING HARDWARE ENHANCEMENTS

It is well known that arcing on the cathode occurs due to the deposition of an insulating layer on the cathode. This insulating layer charges up by ionic bombardment and when the dielectric strength is exceeded, electrical breakdown occurs, leading to arc discharges. Typical dielectric breakdown of Al_2O_3, SiO_2 and SiO occurs at an electric field strength of the order of 10^6 V/cm [5, 10]. It was already shown that arcing is initiated at the transition between the (sputter) cleaned target surface and the contaminated target surface (due to the deposition of oxide). This redeposited oxide layer has a more porous structure than the layer deposited at the substrate which favors the occurrence of arcing [9].

Moving away from the racetrack, the thickness of the redeposited oxide layer first increases and then decreases again (which can be seen at the target tube ends as a change in color of the oxide layer). On the other hand, the plasma fades out in this region and the ionic bombardment diminishes, implying that the charging of the oxide layer decreases with increasing distance from the racetrack. This results in a lower arc rate in areas that are further away from the racetrack compared to areas close to the racetrack. This effect is illustrated in Figure 3. After a short reactive sputter experiment of only 17 minutes the combined effect of the layer thickness and the charging up of the layer results in a clearly visible gradient in arc traces (the concentration of arc traces decreases further away from the racetrack). This is only true at the beginning of the experiment. Later on, the charging of the areas further away from the racetrack increases, as well as the thickness of the redeposited oxide layer, resulting in a higher arc rate in this region too.

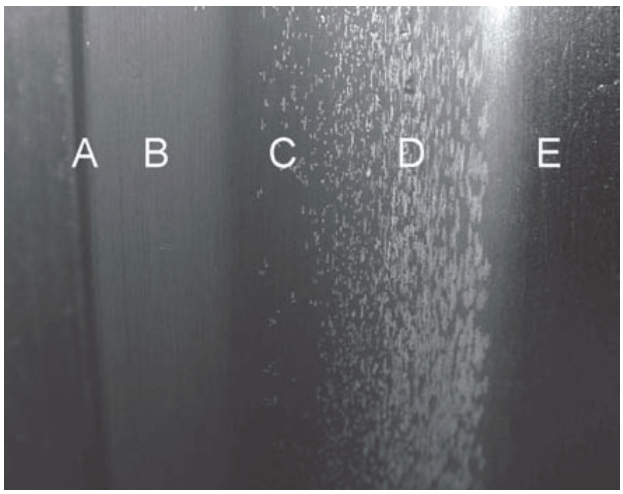

Figure 3. Gradient of arc traces at the target tube end after a short reactive sputter experiment: (A) target tube end, (B) screened region, (C) region with low arc rate, (D) region with high arc rate, (E) racetrack area.

The application of a sufficiently thick dielectric layer of good quality in an arc sensitive area can reduce the arc rate significantly. This can be explained as follows: the electric field in an insulating layer of certain thickness on the cathode surface first increases and then saturates with decreasing conductivity [10] and on the other hand, the electric field decreases with increasing layer thickness. This implies that it is possible to apply an insulating layer on the arc sensitive areas in such a way (carefully chosen properties and thickness) that the electrical field in this insulating layer will never exceed the value of its own breakdown field (the measured value of the electrical breakdown field for typical insulating materials are in the range from 10^5 to 10^7 V/cm [10]). The charging effect of the insulating layer due to ionic bombardment is still taking place, but will not lead to any arc initiation. At the start of the sputter run, when no oxide layer is deposited yet on the dielectric anti-arcing material, the voltage drop falls completely over the protective anti-arcing layer. With increasing redeposited oxide thickness (a low quality oxide layer on top of the dielectric layer) the voltage drop over the oxide layer increases (the stack of oxide on top of an dielectric layer can be viewed as two capacitors in series). The protective dielectric layer is only partially taking care of the voltage drop now and with an improper choice of protective anti-arcing layer (especially during long sputter runs), the redeposited oxide layer may reach dielectric breakdown. Therefore, it is clear that the protective dielectric layer should be chosen and applied with great care. In order to be successful, the dielectric layer should be stable under given (industrial) conditions, which means that the layer should be able to resist high current densities, high temperatures and UV radiation. Besides being a good dielectric material, the layer should be sufficiently thick, sufficiently dense and preferentially amorphous (no grain boundaries which promote dielectric breakdown). This layer should also have a slow sputter rate.

Basis research was already carried out on laboratory scale (small lab coater with 50 mm diameter Al target and DC power of 50 to 300 W) and showed very promising results [9]. Different types of anti-arcing dielectric material were tested and applied in a variety of ways. The arc-inhibiting quality of the layer depends not only on the specific material but also on the way of application. It was shown that the application of a dielectric layer on arc sensitive areas could reduce the arc rate significantly leading to a more stable sputter process.

The upscaling of the results to (semi-)industrial scale using power densities comparable to the ones used in real production environments is however not straightforward. Due to the much higher power densities and the longer sputter runs (resulting in a longer exposure of the dielectric layer to the plasma) the demands on the dielectric layer are even more stringent. Besides the exact type of material and way of application, it was found that the exact position of the dielectric anti-arcing material is extremely critical. With a fixed magnet array position and power, an optimal position for the dielectric material can be determined. If the width of the dielectric protective layer is to small, arcing will initiate at the non-coated parts; if the layer is too broad, the edges of the dielectric anti-arcing layer will start to disintegrate which will lead to severe arcing.

In Figure 4 the arc rate during reactive sputtering of Al_2O_3 is given as a function of time for different treatments of the target tube ends (no dielectric protective layer, a non-optimal dielectric layer and an optimized dielectric layer). The experiment without protective layer was discontinued prematurely because of severe arcing. During all these experiments the arc suppressing unit was set in a way that all arcs (major and minor) were counted. Since the exact number of arcs counted strongly depends on the setting of the arc suppressing unit, arbitrary units were used in Figure 4. It is quite clear from this figure that with a correct choice of protective layer the experiments with a pre-treated target were much more stable and less arcing occurred. With the application of a dielectric anti-arcing layer arcing can be alleviated to a great extent.

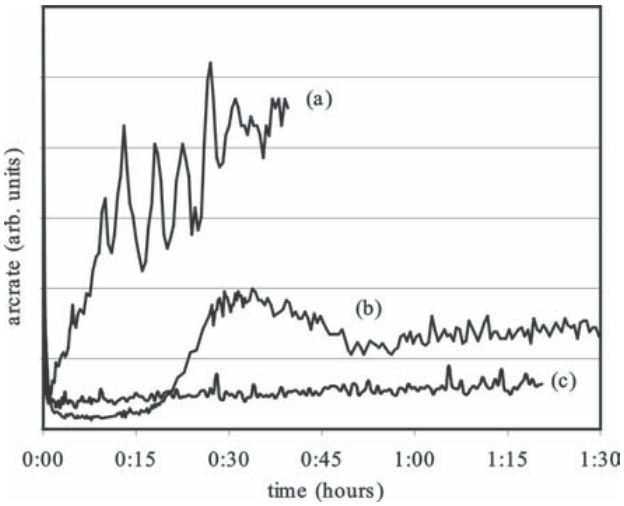

Figure 4. Arc rate as a function of reactive sputter time for different treatments of the target tube ends: (a) no dielectric layer, (b) non-optimized dielectric layer, (c) optimized dielectric layer.

Since arc counting started immediately after introduction of oxygen in the system, the steep rise and subsequent drop in arc rate during the first minute can be attributed to process stabilization effects. The maximum which occurs in the arc rate for the non-optimized coating (b) however cannot be explained yet. Although extremely stable results with drastically reduced arc rates were obtained already, additional experiments will be performed to further optimize the arc inhibiting properties of the dielectric coating and to give a better comprehension of the arcing process.

Although the application of the dielectric anti-arcing layer can be incorporated in the target production process, the use of this layer is a rather unpractical solution and can be quite cumbersome for industrial large-scale operation. Despite the fact that the magnet array position can be adjusted, the exact positioning and exact width of the dielectric layer stays critical, moreover because the exact width depends on the power used during sputtering. Therefore a more practical and more flexible alternative is proposed. In this alternative, an adjustable anti-arcing guard ring (a ring shaped part of the clamping system) replaces the dielectric layer, which is deposited directly on the target surface. This is schematically shown in Figure 5.

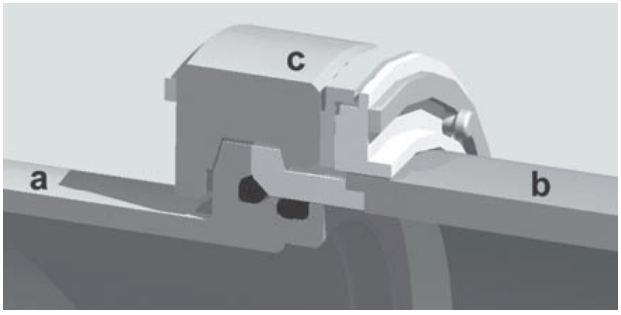

Figure 5. Schematic representation of the anti-arcing guard ring for rotating cylindrical target: (a) magnetron spindle, (b) cylindrical target tube, (c) target clamping with dielectric ring for arc prevention.

IMPROVED ARC-HANDLING ELECTRONICS

Despite all the efforts in optimizing the mechanical design, arcing can be minimized but it is impossible to avoid it completely. Arc-handling electronics is an essential part of the electrical sputter hardware and in particularly indispensable during reactive sputtering of insulating materials. Different components are presented, comprising a compact 2*100 kW power supply, an arc suppressing unit and a low frequency (below 1 kHz) switching unit.

Power Supply

The newly designed power supply excels by its compact size and its superior arc handling capabilities. The compact size is realized by putting a 20 kHz switching system in the primary circuitry, corresponding with a small transformer. The superior arc handling capabilities compared to standard existing power supplies is illustrated in Figure 6.

In this figure, the current and voltage reaction of both newly designed and existing power supply is shown on a bipolar arc event during reactive sputtering (± 20 kW from a single rotating target). No additional arc suppressing electronics were used during this experiment. When the arc occurs (at about 7 ms) the current of the existing power supply starts to rise up to more than 200 A. After a waiting period, the power supply is switched off until the current has dropped below 20 A (this takes more than 100 ms). When the system restarts again a large voltage peak is generated (not shown in this figure) because the plasma is not ignited yet. All this will result in inhomogeneities in the deposited layer (due to the long off period of the power supply) but can also cause severe damage to the target, the substrate and the power supply. With the in-house developed power supply, the current and voltage are tightly controlled so no excessive rise or drop can occur. During the delay after an arc event (before the output of the power supply is stopped) there is only a very small current rise and on reignition of the plasma, no voltage overshoot is generated. Moreover the power supply restarts within 5 ms

after blocking the output. The risk of inhomogeneities in the deposited layer or damage to the substrate, target or power supply is hereby virtually eliminated.

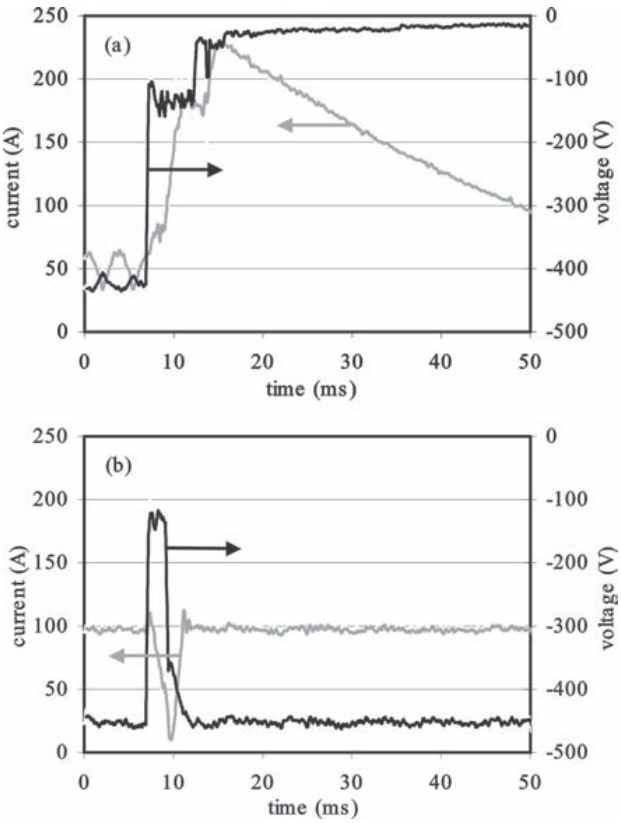

Figure 6. Electrical I-V behavior of an existing (a) and the new in-house developed (b) DC power supply on a bipolar arc (no additional arc suppressing electronics used).

Arc Suppressor

The in-house developed arc suppressing unit is based on the same enhanced technology as the DC power supply. In Figure 7, the current-voltage reaction of an existing DC power supply combined with the superior in-house developed arc suppressing unit on a bipolar arc event is illustrated (note the difference in time scale with Figure 6).

For this experiment a pre-delay time of a few µs was set (pre-delay time can be set from a few µs up to 15 µs). The enhanced arc suppressing unit limits the current rise. Initially, the power supply is shorted by the arc- suppressing unit for about 150 µs after which the power level is brought back to its nominal value in a controlled way, minimizing the voltage overshoot (which occurs when the nominal power is delivered at once to the cathode without plasma). If the arc still exists after these 150 µs, the arc suppressing unit repeats this short procedure (if necessary up to five times). For persistent arcs, which cannot be extinguished by the repeated short procedure, the off time is first increased and eventually, if necessary, the arc suppressor can give a signal to the DC power supply to shut down.

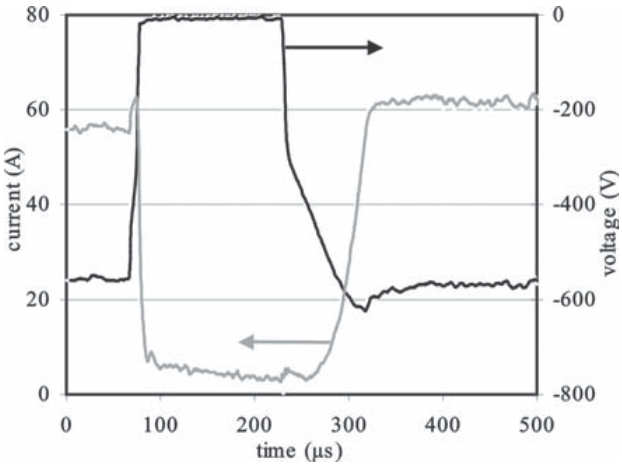

Figure 7. Electrical I-V reaction on a bipolar arc of an existing DC power supply, combined with the new in-house developed arc suppressing unit.

Low Frequency Switcher

Although a switching unit is not an arc-inhibiting device as such, mid-frequency switching between two cathodes is a well-established technique in industry to prevent arcing. The high switching frequencies (10 to 100 kHz) are chosen to discharge the cathodes completely before arcing can occur. However, a lot of time is lost during plasma ignition (e.g. at 40 kHz up to 20%), reducing the deposition rate. On the other hand, mid-frequency switching implies the need for precautions because of electromagnetic radiation and skin effect causing power losses and excessive heating. The problems due to skin effect or electromagnetic radiation are no longer under discussion when low frequency switching (frequency between 50 and 200 Hz) is used and the time lost due to plasma ignition is also negligible. This means that higher power densities can be used resulting in an increased yield. However, because the switching frequency is too low for appropriate arc handling, the low frequency switching unit is combined with the newly designed arc suppressing unit. This combination was tested during reactive AC switching between two full sized rotating cylindrical magnetrons. Good results (long term stability and higher deposition rates as compared to mid-frequency switching) were obtained for most materials.

Important to note is that both the arc suppressing unit and the low frequency switching unit can be linked up with other commercially available power supplies to create a system with superior performance.

CONCLUSIONS

Different ways for preventing and suppressing arc events were discussed. An arc-inhibiting dielectric layer is proposed which is applied directly on the cathode surface onto the arc sensitive areas (the target tube ends for a rotating cylindrical target). This protective layer prevents the redeposited oxide layer from reaching dielectric breakdown. It was shown that arcing during reactive sputter deposition of dielectric layers could be reduced considerably.

Newly designed arc-handling electronics comprising a compact 2*100 kW power supply, an arc suppressing unit and a low-frequency switching unit are proposed. Drastically increased process stability and increased layer homogeneity are obtained. The risk for damage of substrate, target or power supply could be alleviated to a great extent.

The combination of the anti-arcing hardware enhancements and the improved arc-handling electronics provide us with a drastically increased process stability.

ACKNOWLEDGEMENTS

The authors wish to thank the Flemish Community (IWT) for their financial support (IWT 990228).

REFERENCES

1. J. Sellers, "Asymmetric bipolar pulsed DC: the enabling technology for reactive PVD," *Surf. Coat. Technol.*, 98, 1245, 1998.

2. J. Hillendahl, and R. Newcomb, "Utilization of Silicon Targets for Reactive Sputtering From a Rotating Cylindrical DC Magnetron Cathode," *SVC 36th Annual Technical Conference Proceedings*, 491, 1993.

3. I. Safi, "A novel reactive magnetron sputtering technique for producing insulating oxides of metal alloys and other compound thin films," *Surf. Coat. Technol*., 135, 48, 2000.

4. W.D. Sproul, M.E. Graham, M.S. Wong, S. Lopez, D. Li, and R.A. Scholl, "Reactive direct current magnetron sputtering of aluminum oxide coatings," *J. Vac. Sci. Technol*., A13(3), 1188, 1995.

5. A. Belkind, A. Freilich, and R. Scholl, "Pulse duration effects in pulse-power reactive sputtering of Al_2O_3," *Surf. Coat. Technol.*, 108-109, 558, 1998.

6. P.J. Kelly, P.S. Henderson, R.D. Arnell, G.A. Roche, and D. Carter, "Reactive pulsed mangetron sputtering process for alumina films," *J. Vac. Sci. Technol*., A18(6), 2890, 2000.

7. A. Belkind, A. Freilich, and R. Scholl, "Using pulsed direct current power for reactive sputtering of Al_2O_3," *J. Vac. Sci. Technol.*, A17(4), 1934, 1999.

8. K. Koski, J. Hölsä, and P. Juliet, "Surface defects and arc generation in reactive magnetron sputtering of aluminium oxide thin films," *Surf. Coat. Technol*., 115, 163, 1999.

9. W. De Bosscher, G. Gobin, and R. De Gryse, "Global solution of reactive magnetron sputtering," *Proc. 3rd Int. Conf. on Coatings on Glass*, 59, 2000.

10. J. Szczyrbowski, G. Bräuer, W. Dicken, M. Scherer, W. Maass, G. Teschner, and A. Zmelty, "Reactive sputtering of dielectric layers on large scale substrates using an AC twin magnetron cathode," *Surf. Coat. Technol*., 93, 14, 1997.

2001
44th SVC Technical Conference Proceedings

Plenary Session

Process Control & Instrumentation

Decorative & Functional Coating

Emerging Technologies

Joint Vacuum Web/Optical Coating

Large Area Coating

Optical Coating

Plasma Processing

Tribological & Wear Coating

Vacuum Web Coating

2001 continued ...

Vendor Session

Society of Vacuum Coaters Technical Conference Proceedings, CD-ROM 1991-2010 Edition

Copyright Information

Contact SVC at:
e-mail: publications@svc.org
or call: 505/856-7188

Provide your contact information (name, company name and address, phone number and e-mail address) and reference the paper name, paper number and author's last name in your request.

Email: svcinfo@svc.org Web Site: www.svc.org

ISSN 0737-592T
ISBN: 978-1-878068-30-9

Published for the Society of Vacuum Coaters (SVC) by Computer Multimedia Productions Corporation

Appendix 1059

Reactive pulsed magnetron sputtering process for alumina films

Cite as: Journal of Vacuum Science & Technology A **18**, 2890 (2000); https://doi.org/10.1116/1.1319679
Submitted: 17 March 2000 . Accepted: 28 August 2000 . Published Online: 10 November 2000

P. J. Kelly, P. S. Henderson, R. D. Arnell, G. A. Roche, and D. Carter

Reactive pulsed magnetron sputtering process for alumina films

P. J. Kelly,[a] P. S. Henderson, and R. D. Arnell
Centre for Advanced Materials and Surface Engineering, University of Salford, Salford, M5 4WT, United Kingdom

G. A. Roche and D. Carter
Advanced Energy Industries Inc., Fort Collins, Colorado 80525

(Received 17 March 2000; accepted 28 August 2000)

The pulsed magnetron sputtering (PMS) process is now among the leading techniques for the deposition of oxide films. In particular, the use of pulsed dc power has transformed the deposition of dielectric materials, such as alumina. The periodic target voltage reversals during the PMS process effectively discharge poisoned regions on the target. This significantly reduces the occurrence of arc events at the target and stabilizes the deposition process. Many researchers have now shown that pulsed dc reactive magnetron sputtering can be routinely used to produce fully dense, defect-free oxide films. Despite the success of the PMS process, few detailed studies have been carried out on the role played by parameters such as pulse frequency, duty cycle, and reverse voltage in the deposition process. In this study, therefore, alumina films were deposited by reactive pulsed dc magnetron sputtering. Operating conditions were systematically varied and the deposition process monitored throughout. The aim was to investigate the influence of the pulse parameters on the deposition process, and the interrelationships between the occurrence of arc events and the parameters chosen. As a result of this investigation, optimum conditions for the production of high-quality alumina films under hard arc-free conditions were also identified. © *2000 American Vacuum Society.* [S0734-2101(00)04806-5]

I. INTRODUCTION

Since the initial development work in the early 1990s,[1–4] the pulsed magnetron sputtering (PMS) process has become established as one of the leading techniques for the deposition of oxide films. In particular, the use of pulsed dc power has transformed the deposition of dielectric materials, such as alumina.[1–3,5–9] The process itself has been well described in various review articles,[3,6,8–14] and no repetition is required here. It is sufficient to state that pulsed dc reactive magnetron sputtering offers significant advantages over conventional, continuous dc processing.[14] If the magnetron discharge is pulsed in the bipolar mode (see Fig. 1) at frequencies, usually, in the range 10–200 kHz, the periodic target voltage reversals effectively discharge poisoned regions on the target. This significantly reduces the occurrence of arc events at the target and stabilizes the deposition process. Many researchers have now shown that pulsed dc reactive magnetron sputtering can be routinely used to produce fully dense, defect-free oxide films. All stoichiometries are available,[5,6,8] arc events are suppressed,[1–3,6–9,15–17] deposition rates can approach those obtained for metallic films,[2,3,7,15,16] and in dual-cathode systems, very long-term (>300 h) process stability is attainable.[18,19] As a consequence, very significant improvements have been observed in the structure,[5,7,8] hardness,[7,8] and optical properties[6,13] of PMS alumina films, compared to dc sputtered films.

The target voltage wave form during asymmetric bipolar pulsed dc sputtering is shown schematically in Fig. 1. Referring to Fig. 1, the critical parameters which make up the wave form are the pulse frequency, duty factor, and reverse voltage. Duty factor is the relative proportion of the pulse cycle made up of the ''pulse-on'' period, when the target voltage is negative and sputtering is occurring. The reverse voltage is the nominal positive target voltage achieved during the ''pulse-off'' period, often expressed as a percentage of the mean-negative voltage during the pulse-on period. The schematic wave form in Fig. 1 shows a pulse frequency of 100 kHz, with a duty factor of 80%, and the reverse voltage set at 20% of the pulse-on voltage. In practice, this ''square'' wave form is not achieved due to the inherent characteristics of the plasma and the power delivery system, with both positive and negative voltage overshoots being observed.[20] These artifacts can be clearly seen in Fig. 2, an oscilloscope trace of the target voltage wave form obtained when actually operating under the conditions defined previously.

Reference has already been made to the many examples in the literature of the success of the PMS process. However, as yet, few detailed studies have been published on the role played by the pulse parameters in the deposition process. Belkind, Freilich, and Scholl,[9,10] derived an expression showing that the critical pulse frequency for arc-free operation depends on the discharge current and the pulse-off time. Although not explicitly stated, their study indicates that, for a given discharge current, the duty factor is actually the most critical parameter in establishing arc-free conditions. Also, these studies did not consider time-dependent effects, since arc counting was only carried out for 3 min per run. In situations where, during each pulse-off cycle, the parameters selected only partially discharge the poisoned regions on the target, a residual charge will accumulate until, eventually,

[a]Electronic mail: p kelly@salford ac uk

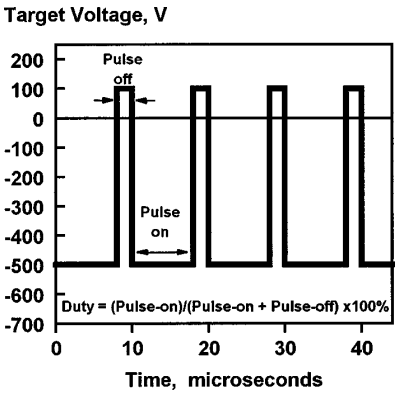

FIG 1 Schematic representation of the target voltage wave form during asymmetric bipolar pulsed sputtering (pulse frequency=100 kHz, reverse time=2 μs, duty=80%, and reverse voltage=20%)

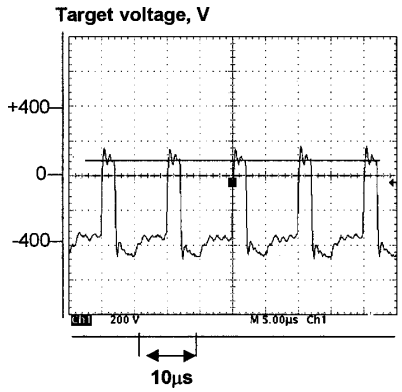

FIG 2 Oscilloscope trace of the target voltage wave form when operating in asymmetric bipolar pulsed mode at 100 kHz (80% duty and 20% reverse voltage)

arcing occurs. Thus, conditions which appear to prevent arcing at the beginning of a deposition run can prove ineffective as the run progresses.

In this study, alumina films were deposited by reactive pulsed dc magnetron sputtering. Operating conditions were systematically varied and the deposition process monitored throughout. The aim was to investigate the influence of the pulse parameters, such as pulse frequency, duty factor, and reverse voltage, and the interrelationships between the occurrence of arc events and the parameters chosen. As a result of this investigation, optimum conditions for the production of high-quality alumina films under hard arc-free conditions were also identified.

II. EXPERIMENT

The commercial interest generated by the PMS process has led to the development of new power delivery systems. These include ac supplies, single- and dual-channel pulsed dc supplies, and pulse units which can be connected in series with the output from standard dc magnetron drivers. This article concentrates on the use of this latter type of system, in which the magnetron discharge could be pulsed over the frequency range 1–100 kHz. Parallel studies are also being made of the latest generation of pulsed dc supply which extends the maximum pulse frequency up to 350 kHz.[21,22]

The dc power supplies used in this study were the Advanced Energy MDX and Pinnacle magnetron drivers. These power supplies were used in conjunction with the Advanced Energy Sparc-le V pulse unit. The Sparc-le V unit allows the pulse parameters to be varied over the following ranges; frequency: 1–100 kHz, reverse time: 1–10 μs, and reverse voltage: 10%–20%. The dc supplies were operated in current regulation mode.

The Sparc-le V unit allows both hard arc and microarc events to be monitored. Hard arcs are generally considered to be a discharge which takes place between a region on the cathode and an earthed surface, whereas microarcs are discharges between different sites on the cathode. While microarcs can normally be tolerated, hard arc events are extremely detrimental to the deposition process.[3,8] Thus, in this study only the incidence of hard arcs was monitored.

The work performed here was carried out in a Teer Coatings Ltd. UDP 450 closed-field unbalanced magnetron sputtering rig, which has been described in detail elsewhere.[7,8] Alumina films were deposited by reactive unbalanced magnetron sputtering from a 99.5% pure Al target. In all cases the base pressure was $<2\times10^{-5}$ mbar, the argon flow rate was adjusted to give a chamber pressure of 2×10^{-3} mbar prior to deposition, and the target current was set to 6 A. The target was precleaned with the substrates shuttered, but no sputter cleaning of the substrates themselves was carried out. In fact, the substrate holder was allowed to float electrically throughout. The flow of reactive gas was controlled by an optical emissions monitoring (OEM) system tuned to the 396 nm line in the Al emission spectrum. An OEM turn-down signal of 25% was used for all depositions, i.e., reactive gas was allowed into the chamber until the OEM signal had fallen to 25% of the initial 100% metal signal. A feedback loop then maintained the OEM signal at this value for the duration of the deposition run, which was typically 90 min. Previous experience had shown that such conditions would produce stoichiometric Al_2O_3 films.[8]

Figure 3 shows the characteristic hysteresis behavior of this system as the oxygen flow rate is varied. As the oxygen flow is increased initially, the target voltage rises slightly. Operating in this ''metallic'' regime could result in the formation of a substoichiometric aluminum oxide film. At a flow rate of approximately 13 sccm of oxygen, the target poisons rapidly and the negative target voltage falls from 395 to 250 V. The target then remains poisoned until the O_2 flow rate is reduced to <4 sccm. Operating in the ''poisoned'' regime would produce stoichiometric films, but at very much reduced deposition rates. The OEM system allows control to be maintained at any point on the hysteresis curve. Figure 4 shows the relationship between target voltage and the OEM setting, expressed as a percentage of the 100% metal signal. As can be seen, operating at a turn-down signal of 25%

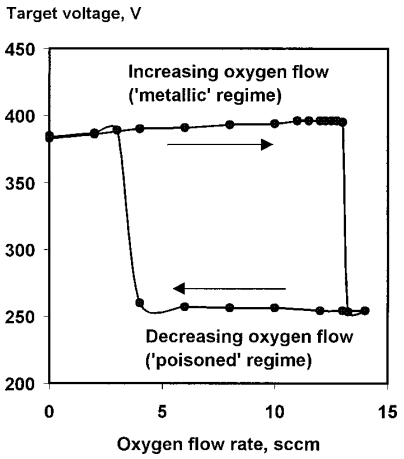

FIG 3 Hysteresis behavior displayed during reactive sputtering of alumina

maintains the target between the metallic and poisoned regimes in a ''partially poisoned'' mode. This allows stoichiometric Al_2O_3 films to be deposited at acceptable rates.

The first stage of this investigation was to deposit a series of alumina films under systematically varied conditions using the Pinnacle/Sparc-le V combination referred to above. For each run, the total number of hard arcs detected by the Sparc-le V was recorded. The film properties were then investigated, and the effectiveness of the deposition conditions at arc suppression was considered. The Taguchi method[23] was used to design this experiment. This method utilizes fractional factorial arrays which are designed to optimize the amount of information obtained from a limited number of experiments, and, as such, it is a very efficient experimental technique. The Taguchi L9 array was selected, which allows up to four factors to be varied at three levels, although only three factors were actually used. The factors chosen were

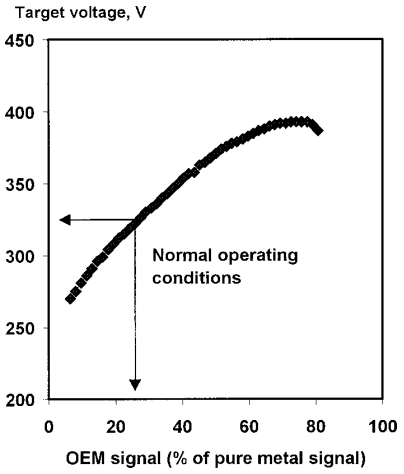

FIG 4 Relationship between optical emission (OEM) signal and target voltage during reactive sputtering of alumina

TABLE I Experimental Taguchi L9 array for the investigation of alumina films

Run No	Pulse frequency (kHz)	Reverse time (μs)	Reverse voltage (%)
1	20	1	10
2	20	5	15
3	20	10	20
4	35	1	15
5	35	5	20
6	35	10	10
7	50	1	20
8	50	5	10
9	50	10	15

pulse frequency (at levels 20, 35, and 50 kHz), reverse time (1, 5, and 10 μs), and reverse voltage (10%, 15%, and 20% of the nominal sputtering voltage). This range of frequencies was chosen because the Sparc-le V limits the maximum reverse time which can be selected at frequencies greater than 50 kHz. Higher frequencies were explored in a second array. The initial experimental array is summarized in Table I.

The alumina films were deposited onto precleaned glass substrates which were subsequently sectioned for analytical purposes. The coating structures were examined by scanning electron microscopy (SEM), with the thickness of each coating being measured from fracture section micrographs. Deposition rates were then calculated from these measurements. The composition of the coatings was determined using a JEOL JXA-50A microanalyzer equipped with WDAX. A high-purity aluminum standard was used in the analysis, with oxygen content being determined by difference. X-ray analyses were carried out using a Philips system, operating in θ–2θ mode (Cu $K\alpha$ radiation), and the resistivity of the coatings was measured using a four-point probe.

Following this, a second array of experiments was carried out. In this case, coatings were deposited over an extended range of pulse frequencies, up to 100 kHz. Also, the MDX magnetron driver was used as the dc supply to allow comparison with the Pinnacle unit. Deposition runs were repeated under, otherwise, identical conditions, but at different levels of duty factor. Care was taken between runs to sputter clean the target, such that all runs started with the target in a similar condition. Run times were varied to ensure that the total pulse-on time was consistent, i.e., the total sputtering time was constant. The reverse voltage was fixed at 20% of the nominal sputtering voltage. The number of hard arcs displayed by the Sparc-le V was recorded at regular intervals, both to monitor the onset of arcing, and to give the total cumulative number of arc events for each set of conditions. The coating structures and properties were investigated as for the preceding array.

III. RESULTS

The deposition rates and total number of hard arcs recorded during each of the Taguchi array runs are listed in Table II. The deposition rates have been normalized to target current to give the rate per minute, per A. The maximum

TABLE II Taguchi L9 array data table

Run No	Duty factor, %	No of hard arcs recorded	Coating thickness (μm)	Normalized dep'n rate (nm/min/A)
1	98	>10 000	4 5	10 0
2	90	1823	3 0	9 3
3	80	5	1 4	4 6
4	96 5	>10 000	2 0	6 5
5	82 5	492	4 0	8 8
6	65	0	0 75	2 3
7	95	>10 000	3 75	11 6
8	75	2754	1 4	4 6
9	50	0	1 8	4 0

number of arcs which can be displayed by the counter on the Sparc-le V is 10 000. Where this value was reached before the end of a run, a value of >10 000 has been inserted in Table II. Also listed in Table II are the duty factors for each run, arising from the array settings of pulse frequency and reverse time. Statistical analyses were carried out on these data using a software package from the American Supplier Institute, entitled ANOVA-TM. This package was used to compute the level averages using deposition rate and number of hard arcs as response variables, i.e., to compute the average response of each variable at each level of each factor. The results of these analyses are shown graphically in Figs. 5 and 7, respectively. It appears from Fig. 5 that reverse time and reverse voltage both have significant, but opposite influences, on deposition rate. In the case of reverse time, this is simply because, as this factor is increased, so the pulse-off time becomes a greater proportion of the total pulse cycle, i.e., the duty factor is reduced and sputtering takes place for a lesser proportion of each cycle. This is illustrated in Fig. 6, which shows the positive correlation between the duty factor and normalized deposition rate (correlation coefficient, r =0.77). Thus, it could be argued that, of the variables investigated, reverse voltage actually has the most significant influence on deposition rate. As reverse voltage is increased from 10% to 20%, the level average for the normalized deposition rate increases from 5.6 to 8.3 nm/min/A, a factor of approximately 1.5 times.

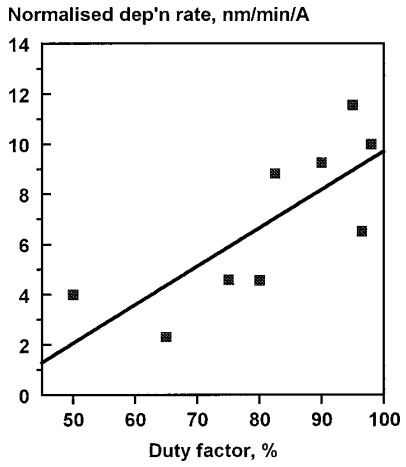

FIG 6 Relationship between the duty factor and normalized deposition rate for reactive pulsed sputtered alumina films

The Taguchi analysis using the total number of hard arcs detected as the response variable is shown in Fig. 7. Rather surprisingly, pulse frequency and reverse voltage do not appear to influence the response variable, whereas the level average for reverse time varies from 10 000 to virtually zero as this parameter is increased from 1 to 10 μs. Clearly, varying the reverse, or pulse-off time can have a very significant

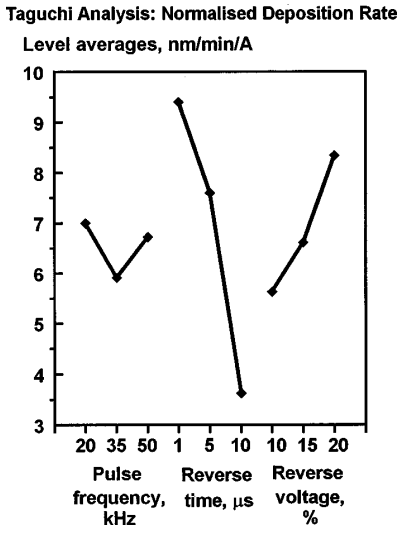

FIG 5 Taguchi analysis of alumina films, using the normalized deposition rate as the response variable

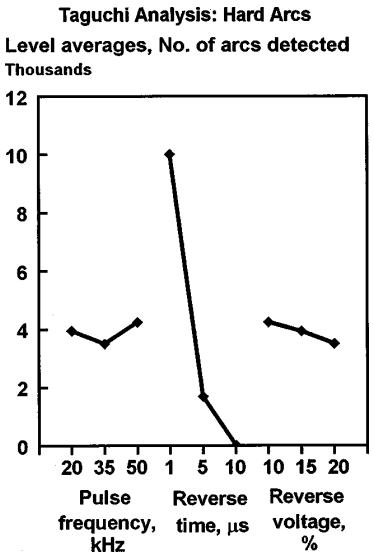

FIG 7 Taguchi analysis of alumina films, using the total number of hard arcs detected as the response variable

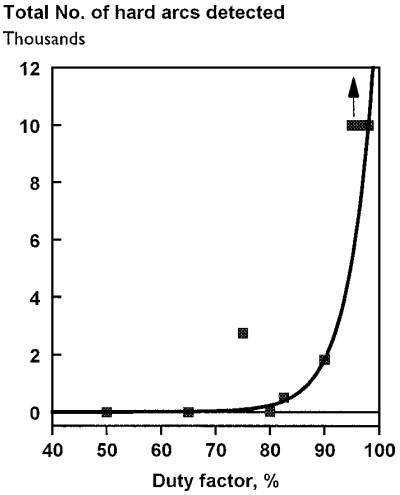

FIG 8 Relationship between the duty factor and the number of hard arcs detected during the deposition of the Taguchi array alumina films

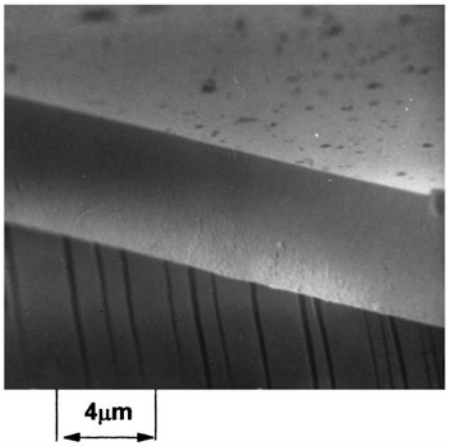

FIG 9 SEM micrograph of the fracture section of an alumina film deposited on a glass substrate: Taguchi array run 1

effect on the occurrence of arc events. Again, though, varying the reverse time has the effect of varying the duty factor. Figure 8, therefore, shows the relationship between the duty factor and the number of arc events recorded for the Taguchi array runs. At duty factors of 95% and higher, greater than 10 000 hard arc events were recorded, independent of the pulse frequency and reverse voltage selected. At lower duty factors the number of arc events decreases exponentially until at 65% and below zero arcs were recorded. At intermediate duty factors, arc events were reduced substantially, but not eliminated. There is some scatter in these data; at a duty factor of 75% the arc count was unexpectedly high compared to the counts at 80% and 82.5% duty. Reference to Table I reveals that in the former case the reverse voltage was set at 10% of the nominal sputtering voltage, whereas in the latter case it was set to 20%. It may, perhaps, be the case that reverse voltage exerts a second-order influence on the occurrence of arcs. This suggestion is merely speculative at this stage. Finally, in these analyses the anticipated interaction between pulse frequency and reverse time was not observed. This may well have been due to the limited range of pulse frequencies investigated.

When the films themselves were examined, very little run-to-run variation was observed. By way of example, Fig. 9 is a SEM micrograph of the fracture section of array coating run 1. In this case, as in all other cases, the coatings were fully dense and defect free, with glass-like featureless structures. Compositional analysis, x-ray diffraction, and four-point probe measurements also showed a consistent pattern. In all cases, within the accuracy of the equipment, the compositions were found to be stoichiometric Al_2O_3. X-ray analysis indicated that these coatings were amorphous. This would be expected, as their deposition temperatures did not exceed 250 °C. Finally, four-point probe measurements confirmed that the coatings were highly insulating. All resistivity readings exceeded 20 MΩ cm, which is the maximum value that could be measured by the probe.

To investigate further the parameters influencing arcing, the second array, described earlier, was carried out. Table III lists the pulse frequencies, reverse times, and duty factors investigated (the reverse voltage was set to 20% throughout). Also included in Table III is the total number of hard arcs displayed by the Sparc-le V at the conclusion of the deposition run. The arc count was also monitored at regular intervals during each run. Figure 10 shows the incidence of arc events during a series of runs carried out at 60 kHz pulse frequency. In these runs, the reverse times were varied from 2 to 6 μs, giving duty factors ranging from 88% to 64%. It is again clear from Fig. 10 that there is a strong relationship between the duty factor and the occurrence of hard arcs. As the duty factor is lowered, the incidence of arcing is significantly reduced. Indeed, at 64% duty, hard arc events were completely suppressed for the duration of the deposition run. At other duty factors there was still an initial arc-free period lasting for several minutes. However, in these cases, charge accumulation eventually reached the point where breakdown occurred. Beyond this point the incidence of arcing increased at an exponential rate.

TABLE III Run conditions and hard arc counts for second alumina array

Run No	Pulse frequency (kHz)	Reverse time (μs)	Duty factor (%)	Total hard arcs detected
1	60	6	64	0
2	60	4	76	37
3	60	3	82	385
4	60	2	87 5	5784
5	20	5	90	1545
6	35	5	82 5	492
7	70	4	72	497
8	80	2	84	3998
9	100	2	80	1041

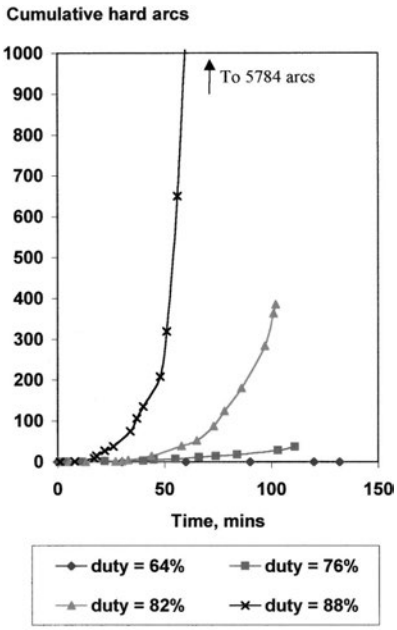

FIG 10 Influence of the duty factor on the incidence of hard arc events during reactive pulsed sputtering of alumina films (pulse frequency=60 kHz)

Overall, the arc counts for the second array were generally lower than those for the Taguchi array. While there may be a number of reasons for this, the second array runs were all carried out at a reverse voltage of 20%. This may, again, be weak evidence that reverse voltage can influence arc suppression.

To confirm that the events recorded by the Sparc-le V unit were indeed arcs, and not merely artifacts of the arc-counting circuitry, the target voltage wave forms were investigated using an oscilloscope. By triggering the oscilloscope on target current, it was possible to capture actual arc events. Figure 11 shows a typical example. At the onset of the arc event, the discharge voltage collapses and the current rises significantly. In this example, it is at least two pulse cycles before the discharge is reestablished.

Coating structures and properties were investigated for the second array coatings, as for the initial array. Again, all coatings were x-ray amorphous with stoichiometric alumina compositions. An example of the structures of these coatings is given in Fig. 12, which shows a SEM micrograph of the fracture section of the coating deposited at 80 kHz (duty =84%). Interestingly, the high number of arcs recorded during the deposition of each of these coatings does not seem to have had a detrimental effect on the structures, which still appear fully dense and defect free. Once again though, further analysis of these films is planned.

IV. DISCUSSION

A number of interesting points have emerged from this investigation. The first Taguchi array demonstrated that over

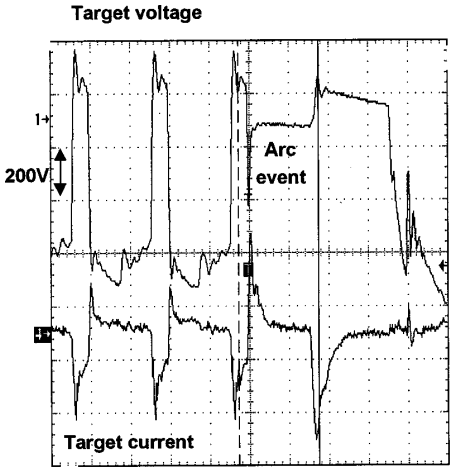

FIG 11 Oscilloscope trace of the target voltage wave form capturing an arc event during pulsed reactive sputtering of alumina films (pulse frequency =100 kHz and duty=80%)

the range tested pulse frequency alone does not significantly influence deposition rate, or the incidence of hard arcs during the deposition of alumina films. The point has already been made that a greater interaction with other parameters might, perhaps, be expected if the range of frequencies was extended. In the case of deposition rate, reverse voltage is the critical factor at any given duty factor. It has been suggested[12] that this may be a result of preferential target cleaning arising from the bipolar nature of the target voltage. At the end of each pulse-off period the target voltage is reversed. At that instant, ions in the vicinity of the target will be accelerated by the normal negative sputtering voltage, plus the positive pulse-off voltage. Thus, at the beginning of each pulse-on period there will be a flux of ions incident at the target with a higher than average energy. Such a flux would preferentially sputter clean poisoned regions of the

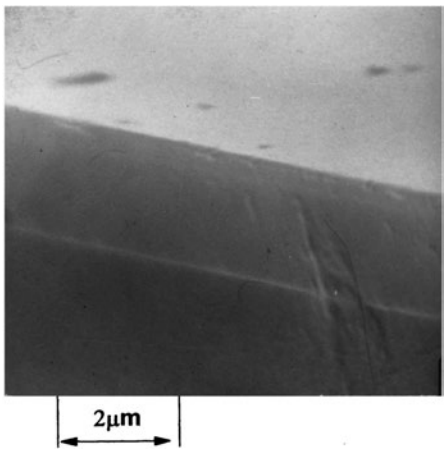

FIG 12 SEM micrograph of an alumina film deposited onto a glass substrate at 80 kHz pulse frequency and 84% duty

target. Since the sputtering rate from a metallic target is higher than the rate from a poisoned target, this would have the effect of raising the deposition rate. Clearly, the effectiveness of the target cleaning would be increased as the magnitude of the reverse voltage is increased, giving rise to the trend observed here. Further studies, including the use of a time-resolved Langmuir probe, are planned to investigate this in more detail.

Both arrays have demonstrated the very strong dependence of hard arc events on the duty factor selected. It appears, therefore, that it would be more appropriate to consider a critical duty factor for arc-free operation, rather than a critical frequency (accepting, again, the limited range of frequencies tested). From these experiments, a duty factor of 70% or lower is necessary, independent of pulse frequency, if arc suppression throughout the duration of a deposition run is the prime concern. The second array did show that limited periods of arc-free operation can be achieved at higher duty factors. This finding is in agreement with Belkind, Freilich, and Scholl,[9,10] who also obtained arc-free reactive sputtering of alumina for short time periods at duties greater than 90%. However, this study indicated that such conditions do not remain arc free and that breakdown soon occurs. Once this has happened, the incidence of arcing then increases at an exponential rate. The scatter observed in the data presented here probably reflects the difficulty in replicating target conditions at the beginning of each run. The target condition is certainly an important, but currently unquantified, factor. Finally, on this subject, and underlining the comments made about the target condition, there may also be some evidence to suggest that increasing the reverse voltage can be beneficial in reducing arcing. In a manner analogous to the influence of reverse voltage on deposition rate, the mechanism for this may again be preferential cleaning of the poisoned regions of the target at the beginning of each pulse-on period. This is somewhat speculative at this stage, and any actual effect is very much second order, compared to the duty factor.

The other surprising point to come out of this work is the apparent insensitivity of the coating structures and properties to the incidence of arcing. The alumina films showed a great deal of similarity at the relatively superficial level of examination used here. All coatings were x-ray amorphous with stoichiometric Al_2O_3 compositions. All structures were fully dense and defect free. More sophisticated analysis of these films is planned for the future, including nanohardness measurements and surface roughness measurements.

To summarize the findings of this work, high-quality alumina films can be deposited by pulsed reactive magnetron sputtering over a broad range of conditions. No significant differences in performance were observed between the two dc magnetron drivers used. The optimum conditions to achieve hard arc-free operation throughout the course of a deposition run, using the power delivery systems and deposition conditions employed here, and for pulse frequencies in the range 20–100 kHz, are to select a duty factor of 70%, with the reverse voltage set to 20%.

V. CONCLUSIONS

High-quality defect-free alumina films have been deposited by pulsed reactive magnetron sputtering over a broad range of conditions. A systematic study of the deposition conditions demonstrated that the incidence of hard arcs is largely controlled by the duty factor selected, and is independent of pulse frequency (over the range tested). It is more appropriate, therefore, to consider the concept of a critical duty factor for arc-free operation, rather than a critical frequency. This study indicates that for the deposition of alumina films a duty factor of 70% or lower is necessary for medium-term (i.e., several hours) arc-free operation. The deposition rate also appeared to be independent of pulse frequency, but to increase with reverse voltage at any given duty factor.

[1]M Scherer, J Schmitt, R Latz, and M Schanz, J Vac Sci Technol A **10**, 1772 (1992)
[2]P Frach, U Heisig, C Gottfried, and H Walde, Surf Coat Technol **59**, 177 (1993)
[3]S Schiller, K Goedicke, J Reschke, V Kirkhoff, S Schneider, and F Milde, Surf Coat Technol **61**, 331 (1993)
[4]D A Glocker, J Vac Sci Technol A **11**, 2989 (1993)
[5]B Stauder, F Perry, and C Frantz, Surf Coat Technol **74-75**, 320 (1995)
[6]W D Sproul, M E Graham, M S Wong, S Lopez, D Li, and R A Scholl, J Vac Sci Technol A **13**, 1188 (1995)
[7]P J Kelly, O A Abu-Zeid, R D Arnell, and J Tong, Surf Coat Technol **86-87**, 28 (1996)
[8]P J Kelly and R D Arnell, J Vac Sci Technol A **17**, 945 (1999)
[9]A Belkind, A Freilich, and R A Scholl, Surf Coat Technol **108-109**, 558 (1998)
[10]A Belkind, A Freilich, and R A Scholl, J Vac Sci Technol A **17**, 1934 (1999)
[11]W D Sproul, Vacuum **51**, 641 (1998)
[12]J C Sellers, Surf Coat Technol **98**, 1245 (1998)
[13]P J Kelly and R D Arnell, Vacuum **56**, 159 (2000)
[14]G Roche and L Mahoney, Vacuum Solutions **12**, 11 (1999)
[15]M S Wong, W J Chia, P Yashar, J M Schneider, W D Sproul, and S A Barnett, Surf Coat Technol **86-87**, 381 (1996)
[16]K Koski, J Holsa, and P Juliet, Surf Coat Technol **116-119**, 716 (1999)
[17]K Koski, J Holsa, and P Juliet, Surf Coat Technol **120-121**, 303 (1999)
[18]G Brauer, J Szczyrbowski, G Teschner, Surf Coat Technol **94-95**, 658 (1997)
[19]G Brauer, M Ruske, J Szczyrbowski, G Teschner, and A Zmelty, Vacuum **51**, 655 (1998)
[20]J M Schneider and W D Sproul, in *Handbook of Thin Film Process Technology: 98/1 Reactive Sputtering*, edited by W D Westwood (IOP, Bristol, 1998)
[21]D Carter, G McDonough, L Mahoney, G A Roche, and H Walde, AVS 46th International Symposium, Seattle, Washington, 25–29 October (1999) (unpublished)
[22]P J Kelly, P S Henderson, R D Arnell, G A Roche, and D Carter, AVS 46th International Symposium, Seattle, Washington, 25–29 October (1999) (unpublished)
[23]R Roy, *A Primer on the Taguchi Method* (Van Nostrand Reinhold, New York, 1990)

Appendix 1059-A

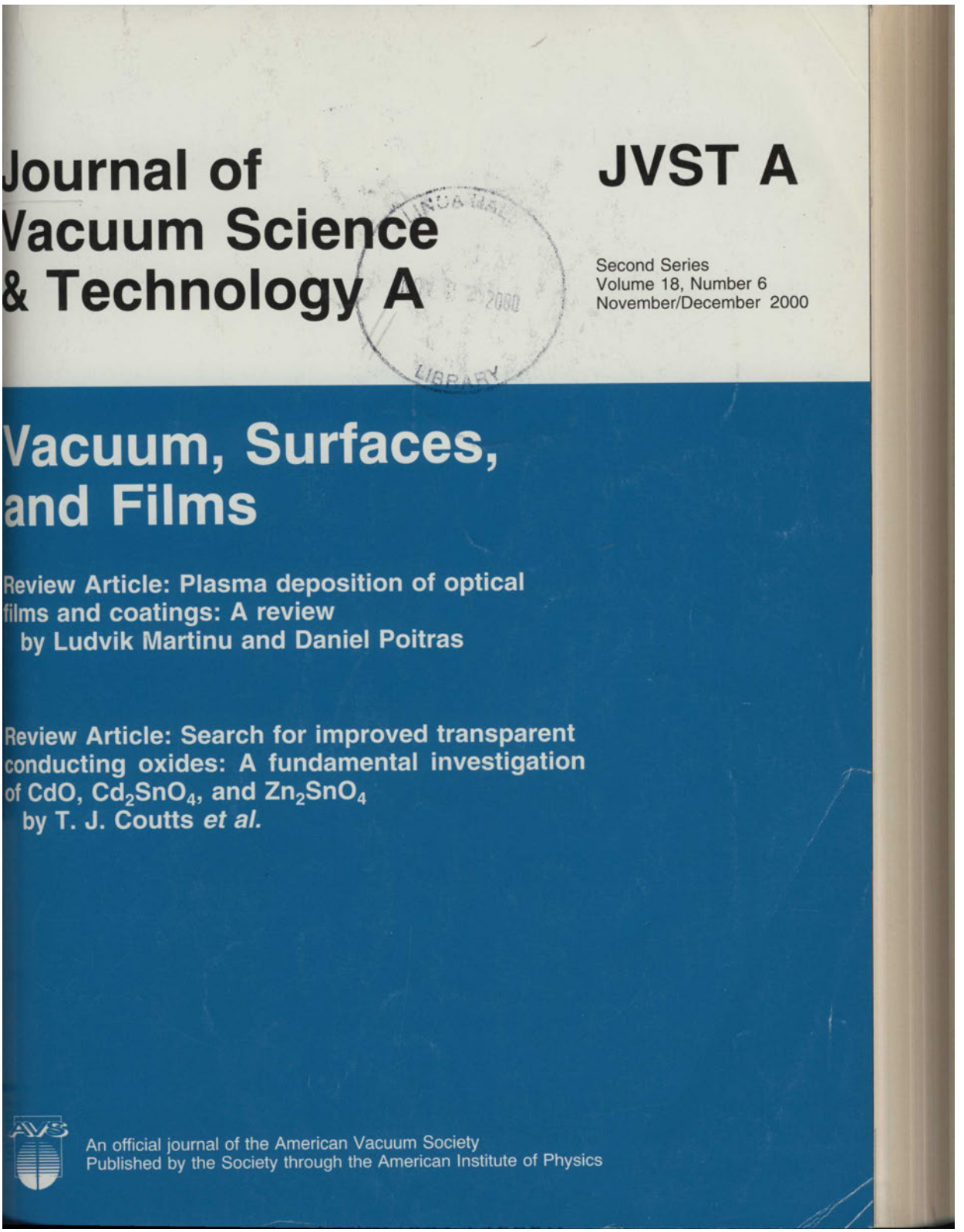
Journal of
Vacuum Science
& Technology A
JVST A
Second Series
Volume 18, Number 6
November/December 2000
LIBRARY
Vacuum, Surfaces,
and Films
Review Article: Plasma deposition of optical films and coatings: A review
by Ludvik Martinu and Daniel Poitras
Review Article: Search for improved transparent conducting oxides: A fundamental investigation of CdO, Cd_2SnO_4, and Zn_2SnO_4
by T. J. Coutts *et al.*
AVS
An official journal of the American Vacuum Society
Published by the Society through the American Institute of Physics


POWER
NOV 2 7 2000
LIBRARY
A&N's new Toggle Clamp design combines strength and speed, producing a superior clamp for the vacuum industry. Machined out of aluminum bar stock, not die-cast, the A&N Toggle clamp has three times the tensile strength of standard industry clamps. Because of its strength, the clamp maintains vacuum integrity even when presented with extreme weight or force. The speed and ease of the closing mechanism save time and eliminate variables in closing torque, producing precise 28° o-ring compression for optimal sealing and extended o-ring life.
For use with QF (ISO-KF) vacuum components
Fast and easy one-step closure
Increased longevity
Proven to withstand a catastrophic blowout
Eliminates the need for an over-pressure ring
Locking pin to prevent accidental opening
...the next evolutionary step in High Vacuum components.
SOME THINGS ARE SIMPLY BUILT BETTER
THE A&N TOGGLE CLAMP
High Vacuum Components Since 1965
A&N CORPORATION
CALL TODAY TOLL-FREE 1-800-FLANGE1
INTERNATIONAL CUSTOMERS CALL (352)528-4100
OR VISIT US ONLINE AT www.ancorp.com
SAME DAY SHIPPING
ORDER TODAY. RECEIVE TOMORROW.
MOST COMPREHENSIVE INVENTORY IN THE INDUSTRY.

Journal of Vacuum Science & Technology A
Vacuum, Surfaces, and Films

JVST A

ISSN: 0734-2101
CODEN: JVTAD6

The Journal of Vacuum Science & Technology A is published six times annually (Jan/Feb, Mar/Apr, May/Jun, Jul/Aug, Sep/Oct, Nov/Dec) by the American Vacuum Society (AVS) through the American Institute of Physics (AIP). It is an official publication of the AVS and is received by all members of the Society. It is devoted to reports of original research and Review articles. The *JVST A* has been established to provide a vehicle for the publication of research dealing with microelectronics and nanometer structures. The emphasis will be on processing, measurement, and phenomena, and will include vacuum processing, plasma processing, materials and structural characterization, microlithography, and the physics and chemistry of submicron and nanometer structures and devices. This journal will publish the proceedings of converences and symposia that are sponsored by the AVS and its divisions.

Submit Manuscripts to the Editorial Office of the *Journal of Vacuum Science & Technology*, 10 Park Plaza, Caller Box 13994, Research Triangle Park, North Carolina 27709-3994; e-mail: jvst@jvst.org. Manuscripts of papers presented at AVS-sponsored conferences and symposia and being submitted to *JVST A* should be sent to the Guest Editor appointed for that particular conference. Before preparing a manuscript, authors should read "Information for Contributors," printed in the first issue of each volume of the journal. Submission of a manuscript is a representation that the manuscript has not been published previously nor currently submitted for publication elsewhere. Upon receipt of a manuscript the Editor will send the author a Transfer of Copyright Agreement form. This must be completed by the author and returned *only* to the Editorial Office prior to publication of an accepted paper in the *Journal of Vacuum Science & Technology A*. This written transfer of copyright, which previously was assumed to be implicit in the act of submitting a manuscript, is necessary under the 1978 copyright law in order for the AVS and AIP to continue disseminating research results as widely as possible. Further information may be obtained from AIP.

Publication Charge: To support the cost of wide dissemination of research results through the publication of journal pages and production of a database of articles, the author's institution is requested to pay a *page charge* of $95 per page (with a one-page minimum). The charge (if honored) entitles the author to 100 free reprints. For Errata the minimum page charge is $10, with no free reprints.

Electronic Physics Auxiliary Publication Service (EPAPS): EPAPS is a low-cost electronic depository for material that is supplemental to a journal article. For a nominal fee, authors may submit multimedia (e.g., movie files, audio files, 3D rendering files), color figures, data tables, etc. Retrieval instructions are footnoted in the related published paper. Direct requests to the Editor; for additional information see http://www.aip.org/pubservs/epaps.html.

Advertising Rates will be supplied on request from AIP's Advertising Division, Suite 1NO1, 2 Huntington Quadrangle, Melville, NY 11747-4502. Telephone: (516) 576-2440. Fax: (516) 576-2481. E-mail: advtsg@aip.org. All insertion orders and advertising material should be sent to that division.

American Vacuum Society

Officers

Paula Grunthaner, *President*
Jet Propulsion Lab, Caltech

Steve Rossnagel, *Immediate Past-President*
IBM T. J. Watson Research Center

Joseph E. Greene, *Secretary*
University of Illinois

John W. Coburn, *Treasurer*
Univ. of CA, Berkeley

Directors

Cammy R. Abernathy
University of Florida

Gregory J. Exarhos
Pacific Northwest National Lab.

Calvin Gabriel
Advanced Micro Devices

Howard Patton
LLNL

Peter M. A. Sherwood
Kansas State University

Dorota Temple
MCNC

JVST

G. Lucovsky, *Editor-in-Chief*
North Carolina State University

AVS Membership Information may be obtained from

Angela Mulligan
AVS Member Services Coordinator
120 Wall Street
32nd Floor
New York, NY 10005
(212) 248-0200
angela@vacuum.org
www.vacuum.org

Journal of Vacuum Science & Technology A

Vacuum, Surfaces, and Films

JVST A

Second Series
Volume 18, Number 6
Nov/Dec 2000

Review Articles

Articles

(Continued)

Journal of Vacuum Science & Technology A (ISSN: 0734-2101) is published six times annually (Jan/Feb, Mar/Apr, May/Jun, Jul/Aug, Sep/Oct, Nov/Dec) by the American Vacuum Society through the American Institute of Physics, Suite 1NO1, 2 Huntington Quadrangle, Melville, NY 11747-4502. 2000 subscription rates are: US$835. POSTMASTER: Send address changes to *Journal of Vacuum Science & Technology A*, SLACK Inc., 6900 Grove Road, Thorofare, NJ 08086. Periodicals postage paid at Thorofare, NJ 08086, and at additional mailing offices.

Membership in the American Vacuum Society includes $17.50 from membership dues to be applied towards a subscription to *Journal of Vacuum Science & Technology A*.

Subscription Prices (2000)

	U.S.A. and Poss.	Can., Mex., Central & S. America & Caribbean	Europe, Asia, Africa & Oceania*
JVST A†	$835	$868	$891
JVST A‡	$960	$990	$1017
JVST A and B†	$960	$1024	$1070
JVST A and B#	$960	$990	$990
JVST A and B‡	$1086	$1150	$1196

†Print and online.
‡Print and CD-ROM.
#CD-ROM only.
*Nonmember subscriptions include air-freight service.

Back-number Prices: 2000 single copies: $155; prior to 2000 single copies: $105.

Subscriptions, renewals, and address changes should be addressed to *Subscription Fullfillment Division, SLACK, Inc., 6900 Grove Road, Thorofare, NJ 08086.* Allow at least six weeks advance notice. For address changes please send both old and new addresses, and, if possible, include a label from the plastic mailing wrapper of a recent issue. Missing issue requests will be honored only if received within six months of publication date (nine months for Australia and Asia).

Single-copy orders (current and back issues) should be addressed to American Institute of Physics, Circulation and Fulfillment Division, Suite 1NO1, 2 Huntington Quadrangle, Melville, NY 11747-4502; Telephone: 800-344-6902 (or 516-576-2230 outside the U.S.A.), Fax at 516-349-9704, or E-mail at subs@aip.org.

Reprints: Reprints can be ordered with or without covers only in multiples of 50 (with a minimum of 100 in each catagory) from AIP, Circulation and Fulfillment/Reprints, Suite 1NO1, 2 Huntington Quadrangle, Melville, NY 11747-4502; Fax: 516-349-9704; Telephone: 800-344-6909 (U.S. and Canada) or 516-576-2230.

Document Delivery: Copies of journal articles can be ordered for online delivery from DocumentStore, AIP's online document delivery service (http://ojs.aip.org/documentstore/).

Microform: *Journal of Vacuum Science & Technology A* is available on microfiche issued at the same frequency as the printed journal and annually on microfilm. Direct requests to AIP, Circulation and Fulfillment/Single Copy Sales, Suite 1NO1, 2 Huntington Quadrangle, Melville, NY 11747-4502, Fax: 516-349-9704; Telephone: 800-344-6908 (U.S. and Canada) or 516-576-2230.

Online Access: The *Journal of Vacuum Science and Technology A* is available online to AVS members at no additional charge; for details, please see http://ojps.aip.org/jvsta/. Abstracts of journal articles are available from AIP's SPIN Web Service (http://ojps.aip.org/spinweb/).

(Continued)

(Continued)

Rapid Communications

Errata

INDEX

Reactive pulsed magnetron sputtering process for alumina films

P. J. Kelly,[a] P. S. Henderson, and R. D. Arnell
Centre for Advanced Materials and Surface Engineering, University of Salford, Salford, M5 4WT, United Kingdom

G. A. Roche and D. Carter
Advanced Energy Industries Inc., Fort Collins, Colorado 80525

(Received 17 March 2000; accepted 28 August 2000)

The pulsed magnetron sputtering (PMS) process is now among the leading techniques for the deposition of oxide films. In particular, the use of pulsed dc power has transformed the deposition of dielectric materials, such as alumina. The periodic target voltage reversals during the PMS process effectively discharge poisoned regions on the target. This significantly reduces the occurrence of arc events at the target and stabilizes the deposition process. Many researchers have now shown that pulsed dc reactive magnetron sputtering can be routinely used to produce fully dense, defect-free oxide films. Despite the success of the PMS process, few detailed studies have been carried out on the role played by parameters such as pulse frequency, duty cycle, and reverse voltage in the deposition process. In this study, therefore, alumina films were deposited by reactive pulsed dc magnetron sputtering. Operating conditions were systematically varied and the deposition process monitored throughout. The aim was to investigate the influence of the pulse parameters on the deposition process, and the interrelationships between the occurrence of arc events and the parameters chosen. As a result of this investigation, optimum conditions for the production of high-quality alumina films under hard arc-free conditions were also identified. © *2000 American Vacuum Society.* [S0734-2101(00)04806-5]

I. INTRODUCTION

Since the initial development work in the early 1990s,[1–4] the pulsed magnetron sputtering (PMS) process has become established as one of the leading techniques for the deposition of oxide films. In particular, the use of pulsed dc power has transformed the deposition of dielectric materials, such as alumina.[1–3,5–9] The process itself has been well described in various review articles,[3,6,8–14] and no repetition is required here. It is sufficient to state that pulsed dc reactive magnetron sputtering offers significant advantages over conventional, continuous dc processing.[14] If the magnetron discharge is pulsed in the bipolar mode (see Fig. 1) at frequencies, usually, in the range 10–200 kHz, the periodic target voltage reversals effectively discharge poisoned regions on the target. This significantly reduces the occurrence of arc events at the target and stabilizes the deposition process. Many researchers have now shown that pulsed dc reactive magnetron sputtering can be routinely used to produce fully dense, defect-free oxide films. All stoichiometries are available,[5,6,8] arc events are suppressed,[1–3,6–9,15–17] deposition rates can approach those obtained for metallic films,[2,3,7,15,16] and in dual-cathode systems, very long-term (>300 h) process stability is attainable.[18,19] As a consequence, very significant improvements have been observed in the structure,[5,7,8] hardness,[7,8] and optical properties[6,13] of PMS alumina films, compared to dc sputtered films.

The target voltage wave form during asymmetric bipolar pulsed dc sputtering is shown schematically in Fig. 1. Referring to Fig. 1, the critical parameters which make up the wave form are the pulse frequency, duty factor, and reverse voltage. Duty factor is the relative proportion of the pulse cycle made up of the "pulse-on" period, when the target voltage is negative and sputtering is occurring. The reverse voltage is the nominal positive target voltage achieved during the "pulse-off" period, often expressed as a percentage of the mean-negative voltage during the pulse-on period. The schematic wave form in Fig. 1 shows a pulse frequency of 100 kHz, with a duty factor of 80%, and the reverse voltage set at 20% of the pulse-on voltage. In practice, this "square" wave form is not achieved due to the inherent characteristics of the plasma and the power delivery system, with both positive and negative voltage overshoots being observed.[20] These artifacts can be clearly seen in Fig. 2, an oscilloscope trace of the target voltage wave form obtained when actually operating under the conditions defined previously.

Reference has already been made to the many examples in the literature of the success of the PMS process. However, as yet, few detailed studies have been published on the role played by the pulse parameters in the deposition process. Belkind, Freilich, and Scholl,[9,10] derived an expression showing that the critical pulse frequency for arc-free operation depends on the discharge current and the pulse-off time. Although not explicitly stated, their study indicates that, for a given discharge current, the duty factor is actually the most critical parameter in establishing arc-free conditions. Also, these studies did not consider time-dependent effects, since arc counting was only carried out for 3 min per run. In situations where, during each pulse-off cycle, the parameters selected only partially discharge the poisoned regions on the target, a residual charge will accumulate until, eventually,

[a]Electronic mail: p.kelly@salford.ac.uk

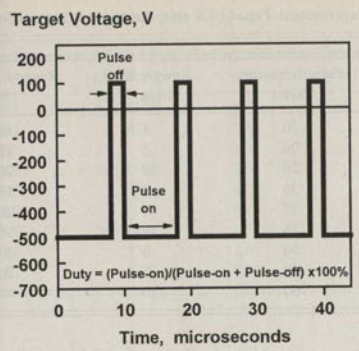

FIG. 1. Schematic representation of the target voltage wave form during asymmetric bipolar pulsed sputtering (pulse frequency=100 kHz, reverse time=2 μs, duty=80%, and reverse voltage=20%).

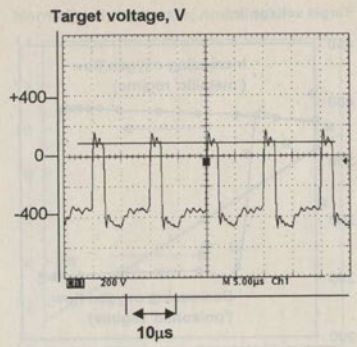

FIG. 2. Oscilloscope trace of the target voltage wave form when operating in asymmetric bipolar pulsed mode at 100 kHz (80% duty and 20% reverse voltage).

arcing occurs. Thus, conditions which appear to prevent arcing at the beginning of a deposition run can prove ineffective as the run progresses.

In this study, alumina films were deposited by reactive pulsed dc magnetron sputtering. Operating conditions were systematically varied and the deposition process monitored throughout. The aim was to investigate the influence of the pulse parameters, such as pulse frequency, duty factor, and reverse voltage, and the interrelationships between the occurrence of arc events and the parameters chosen. As a result of this investigation, optimum conditions for the production of high-quality alumina films under hard arc-free conditions were also identified.

II. EXPERIMENT

The commercial interest generated by the PMS process has led to the development of new power delivery systems. These include ac supplies, single- and dual-channel pulsed dc supplies, and pulse units which can be connected in series with the output from standard dc magnetron drivers. This article concentrates on the use of this latter type of system, in which the magnetron discharge could be pulsed over the frequency range 1–100 kHz. Parallel studies are also being made of the latest generation of pulsed dc supply which extends the maximum pulse frequency up to 350 kHz.[21,22]

The dc power supplies used in this study were the Advanced Energy MDX and Pinnacle magnetron drivers. These power supplies were used in conjunction with the Advanced Energy Sparc-le V pulse unit. The Sparc-le V unit allows the pulse parameters to be varied over the following ranges; frequency: 1–100 kHz, reverse time: 1–10 μs, and reverse voltage: 10%–20%. The dc supplies were operated in current regulation mode.

The Sparc-le V unit allows both hard arc and microarc events to be monitored. Hard arcs are generally considered to be a discharge which takes place between a region on the cathode and an earthed surface, whereas microarcs are discharges between different sites on the cathode. While microarcs can normally be tolerated, hard arc events are extremely detrimental to the deposition process.[3,8] Thus, in this study only the incidence of hard arcs was monitored.

The work performed here was carried out in a Teer Coatings Ltd. UDP 450 closed-field unbalanced magnetron sputtering rig, which has been described in detail elsewhere.[7,8] Alumina films were deposited by reactive unbalanced magnetron sputtering from a 99.5% pure Al target. In all cases the base pressure was $<2\times10^{-5}$ mbar, the argon flow rate was adjusted to give a chamber pressure of 2×10^{-3} mbar prior to deposition, and the target current was set to 6 A. The target was precleaned with the substrates shuttered, but no sputter cleaning of the substrates themselves was carried out. In fact, the substrate holder was allowed to float electrically throughout. The flow of reactive gas was controlled by an optical emissions monitoring (OEM) system tuned to the 396 nm line in the Al emission spectrum. An OEM turn-down signal of 25% was used for all depositions, i.e., reactive gas was allowed into the chamber until the OEM signal had fallen to 25% of the initial 100% metal signal. A feedback loop then maintained the OEM signal at this value for the duration of the deposition run, which was typically 90 min. Previous experience had shown that such conditions would produce stoichiometric Al_2O_3 films.[8]

Figure 3 shows the characteristic hysteresis behavior of this system as the oxygen flow rate is varied. As the oxygen flow is increased initially, the target voltage rises slightly. Operating in this "metallic" regime could result in the formation of a substoichiometric aluminum oxide film. At a flow rate of approximately 13 sccm of oxygen, the target poisons rapidly and the negative target voltage falls from 395 to 250 V. The target then remains poisoned until the O_2 flow rate is reduced to <4 sccm. Operating in the "poisoned" regime would produce stoichiometric films, but at very much reduced deposition rates. The OEM system allows control to be maintained at any point on the hysteresis curve. Figure 4 shows the relationship between target voltage and the OEM setting, expressed as a percentage of the 100% metal signal. As can be seen, operating at a turn-down signal of 25%

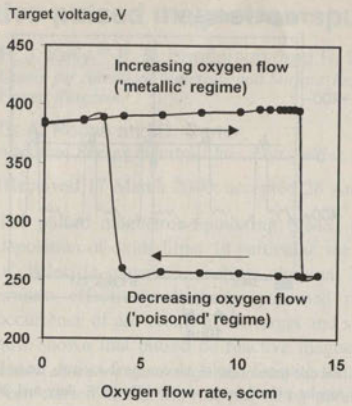

FIG. 3. Hysteresis behavior displayed during reactive sputtering of alumina.

maintains the target between the metallic and poisoned regimes in a ''partially poisoned'' mode. This allows stoichiometric Al_2O_3 films to be deposited at acceptable rates.

The first stage of this investigation was to deposit a series of alumina films under systematically varied conditions using the Pinnacle/Sparc-le V combination referred to above. For each run, the total number of hard arcs detected by the Sparc-le V was recorded. The film properties were then investigated, and the effectiveness of the deposition conditions at arc suppression was considered. The Taguchi method[23] was used to design this experiment. This method utilizes fractional factorial arrays which are designed to optimize the amount of information obtained from a limited number of experiments, and, as such, it is a very efficient experimental technique. The Taguchi L9 array was selected, which allows up to four factors to be varied at three levels, although only three factors were actually used. The factors chosen were

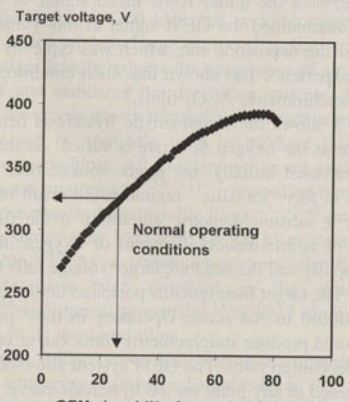

FIG. 4. Relationship between optical emission (OEM) signal and target voltage during reactive sputtering of alumina.

TABLE I. Experimental Taguchi L9 array for the investigation of alumina films.

Run No.	Pulse frequency (kHz)	Reverse time (μs)	Reverse voltage (%)
1	20	1	10
2	20	5	15
3	20	10	20
4	35	1	15
5	35	5	20
6	35	10	10
7	50	1	20
8	50	5	10
9	50	10	15

pulse frequency (at levels 20, 35, and 50 kHz), reverse time (1, 5, and 10 μs), and reverse voltage (10%, 15%, and 20% of the nominal sputtering voltage). This range of frequencies was chosen because the Sparc-le V limits the maximum reverse time which can be selected at frequencies greater than 50 kHz. Higher frequencies were explored in a second array. The initial experimental array is summarized in Table I.

The alumina films were deposited onto precleaned glass substrates which were subsequently sectioned for analytical purposes. The coating structures were examined by scanning electron microscopy (SEM), with the thickness of each coating being measured from fracture section micrographs. Deposition rates were then calculated from these measurements. The composition of the coatings was determined using a JEOL JXA-50A microanalyzer equipped with WDAX. A high-purity aluminum standard was used in the analysis, with oxygen content being determined by difference. X-ray analyses were carried out using a Philips system, operating in θ–2θ mode (Cu $K\alpha$ radiation), and the resistivity of the coatings was measured using a four-point probe.

Following this, a second array of experiments was carried out. In this case, coatings were deposited over an extended range of pulse frequencies, up to 100 kHz. Also, the MDX magnetron driver was used as the dc supply to allow comparison with the Pinnacle unit. Deposition runs were repeated under, otherwise, identical conditions, but at different levels of duty factor. Care was taken between runs to sputter clean the target, such that all runs started with the target in a similar condition. Run times were varied to ensure that the total pulse-on time was consistent, i.e., the total sputtering time was constant. The reverse voltage was fixed at 20% of the nominal sputtering voltage. The number of hard arcs displayed by the Sparc-le V was recorded at regular intervals, both to monitor the onset of arcing, and to give the total cumulative number of arc events for each set of conditions. The coating structures and properties were investigated as for the preceding array.

III. RESULTS

The deposition rates and total number of hard arcs recorded during each of the Taguchi array runs are listed in Table II. The deposition rates have been normalized to target current to give the rate per minute, per A. The maximum

TABLE II. Taguchi L9 array data table.

Run No.	Duty factor, %	No. of hard arcs recorded	Coating thickness (μm)	Normalized dep'n rate (nm/min/A)
1	98	>10 000	4.5	10.0
2	90	1823	3.0	9.3
3	80	5	1.4	4.6
4	96.5	>10 000	2.0	6.5
5	82.5	492	4.0	8.8
6	65	0	0.75	2.3
7	95	>10 000	3.75	11.6
8	75	2754	1.4	4.6
9	50	0	1.8	4.0

number of arcs which can be displayed by the counter on the Sparc-le V is 10 000. Where this value was reached before the end of a run, a value of >10 000 has been inserted in Table II. Also listed in Table II are the duty factors for each run, arising from the array settings of pulse frequency and reverse time. Statistical analyses were carried out on these data using a software package from the American Supplier Institute, entitled ANOVA-TM. This package was used to compute the level averages using deposition rate and number of hard arcs as response variables, i.e., to compute the average response of each variable at each level of each factor. The results of these analyses are shown graphically in Figs. 5 and 7, respectively. It appears from Fig. 5 that reverse time and reverse voltage both have significant, but opposite influences, on deposition rate. In the case of reverse time, this is simply because, as this factor is increased, so the pulse-off time becomes a greater proportion of the total pulse cycle, i.e., the duty factor is reduced and sputtering takes place for a lesser proportion of each cycle. This is illustrated in Fig. 6, which shows the positive correlation between the duty factor and normalized deposition rate (correlation coefficient, r =0.77). Thus, it could be argued that, of the variables investigated, reverse voltage actually has the most significant influence on deposition rate. As reverse voltage is increased from 10% to 20%, the level average for the normalized deposition rate increases from 5.6 to 8.3 nm/min/A, a factor of approximately 1.5 times.

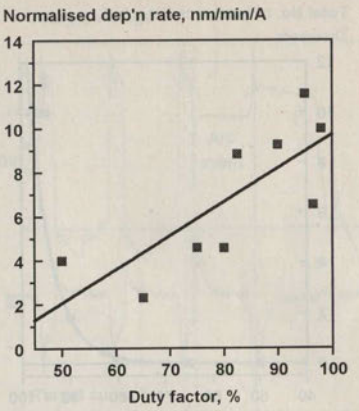

FIG. 6. Relationship between the duty factor and normalized deposition rate for reactive pulsed sputtered alumina films.

The Taguchi analysis using the total number of hard arcs detected as the response variable is shown in Fig. 7. Rather surprisingly, pulse frequency and reverse voltage do not appear to influence the response variable, whereas the level average for reverse time varies from 10 000 to virtually zero as this parameter is increased from 1 to 10 μs. Clearly, varying the reverse, or pulse-off time can have a very significant

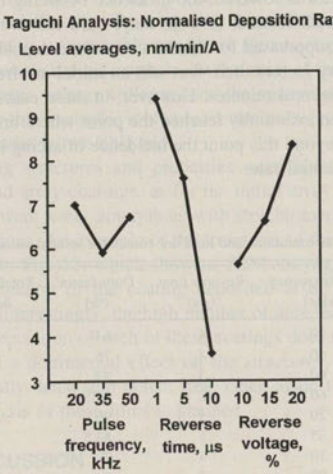

FIG. 5. Taguchi analysis of alumina films, using the normalized deposition rate as the response variable.

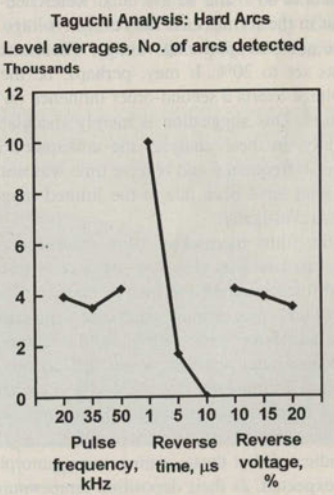

FIG. 7. Taguchi analysis of alumina films, using the total number of hard arcs detected as the response variable.

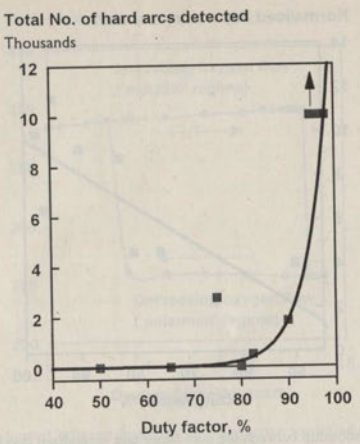

FIG. 8. Relationship between the duty factor and the number of hard arcs detected during the deposition of the Taguchi array alumina films.

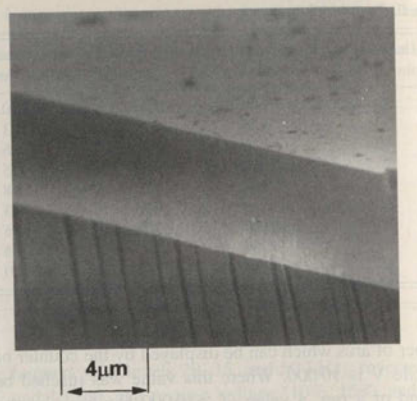

FIG. 9. SEM micrograph of the fracture section of an alumina film deposited on a glass substrate: Taguchi array run 1.

effect on the occurrence of arc events. Again, though, varying the reverse time has the effect of varying the duty factor. Figure 8, therefore, shows the relationship between the duty factor and the number of arc events recorded for the Taguchi array runs. At duty factors of 95% and higher, greater than 10 000 hard arc events were recorded, independent of the pulse frequency and reverse voltage selected. At lower duty factors the number of arc events decreases exponentially until at 65% and below zero arcs were recorded. At intermediate duty factors, arc events were reduced substantially, but not eliminated. There is some scatter in these data; at a duty factor of 75% the arc count was unexpectedly high compared to the counts at 80% and 82.5% duty. Reference to Table I reveals that in the former case the reverse voltage was set at 10% of the nominal sputtering voltage, whereas in the latter case it was set to 20%. It may, perhaps, be the case that reverse voltage exerts a second-order influence on the occurrence of arcs. This suggestion is merely speculative at this stage. Finally, in these analyses the anticipated interaction between pulse frequency and reverse time was not observed. This may well have been due to the limited range of pulse frequencies investigated.

When the films themselves were examined, very little run-to-run variation was observed. By way of example, Fig. 9 is a SEM micrograph of the fracture section of array coating run 1. In this case, as in all other cases, the coatings were fully dense and defect free, with glass-like featureless structures. Compositional analysis, x-ray diffraction, and four-point probe measurements also showed a consistent pattern. In all cases, within the accuracy of the equipment, the compositions were found to be stoichiometric Al_2O_3. X-ray analysis indicated that these coatings were amorphous. This would be expected, as their deposition temperatures did not exceed 250 °C. Finally, four-point probe measurements confirmed that the coatings were highly insulating. All resistivity readings exceeded 20 MΩ cm, which is the maximum value that could be measured by the probe.

To investigate further the parameters influencing arcing, the second array, described earlier, was carried out. Table III lists the pulse frequencies, reverse times, and duty factors investigated (the reverse voltage was set to 20% throughout). Also included in Table III is the total number of hard arcs displayed by the Sparc-le V at the conclusion of the deposition run. The arc count was also monitored at regular intervals during each run. Figure 10 shows the incidence of arc events during a series of runs carried out at 60 kHz pulse frequency. In these runs, the reverse times were varied from 2 to 6 μs, giving duty factors ranging from 88% to 64%. It is again clear from Fig. 10 that there is a strong relationship between the duty factor and the occurrence of hard arcs. As the duty factor is lowered, the incidence of arcing is significantly reduced. Indeed, at 64% duty, hard arc events were completely suppressed for the duration of the deposition run. At other duty factors there was still an initial arc-free period lasting for several minutes. However, in these cases, charge accumulation eventually reached the point where breakdown occurred. Beyond this point the incidence of arcing increased at an exponential rate.

TABLE III. Run conditions and hard arc counts for second alumina array.

Run No.	Pulse frequency (kHz)	Reverse time (μs)	Duty factor (%)	Total hard arcs detected
1	60	6	64	0
2	60	4	76	37
3	60	3	82	385
4	60	2	87.5	5784
5	20	5	90	1545
6	35	5	82.5	492
7	70	4	72	497
8	80	2	84	3998
9	100	2	80	1041

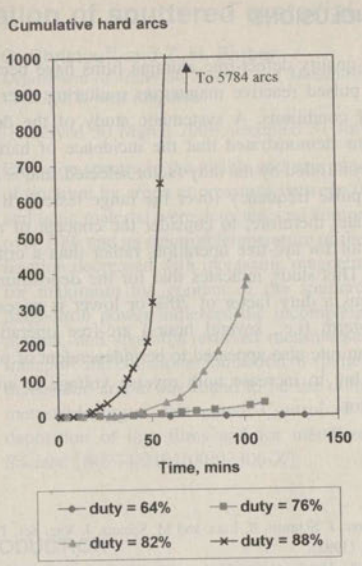

FIG. 10. Influence of the duty factor on the incidence of hard arc events during reactive pulsed sputtering of alumina films (pulse frequency=60 kHz).

Overall, the arc counts for the second array were generally lower than those for the Taguchi array. While there may be a number of reasons for this, the second array runs were all carried out at a reverse voltage of 20%. This may, again, be weak evidence that reverse voltage can influence arc suppression.

To confirm that the events recorded by the Sparc-le V unit were indeed arcs, and not merely artifacts of the arc-counting circuitry, the target voltage wave forms were investigated using an oscilloscope. By triggering the oscilloscope on target current, it was possible to capture actual arc events. Figure 11 shows a typical example. At the onset of the arc event, the discharge voltage collapses and the current rises significantly. In this example, it is at least two pulse cycles before the discharge is reestablished.

Coating structures and properties were investigated for the second array coatings, as for the initial array. Again, all coatings were x-ray amorphous with stoichiometric alumina compositions. An example of the structures of these coatings is given in Fig. 12, which shows a SEM micrograph of the fracture section of the coating deposited at 80 kHz (duty =84%). Interestingly, the high number of arcs recorded during the deposition of each of these coatings does not seem to have had a detrimental effect on the structures, which still appear fully dense and defect free. Once again though, further analysis of these films is planned.

IV. DISCUSSION

A number of interesting points have emerged from this investigation. The first Taguchi array demonstrated that over

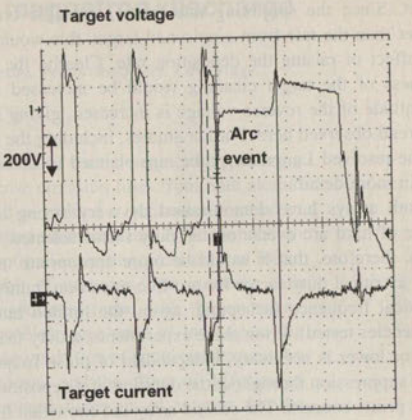

FIG. 11. Oscilloscope trace of the target voltage wave form capturing an arc event during pulsed reactive sputtering of alumina films (pulse frequency =100 kHz and duty=80%).

the range tested pulse frequency alone does not significantly influence deposition rate, or the incidence of hard arcs during the deposition of alumina films. The point has already been made that a greater interaction with other parameters might, perhaps, be expected if the range of frequencies was extended. In the case of deposition rate, reverse voltage is the critical factor at any given duty factor. It has been suggested[12] that this may be a result of preferential target cleaning arising from the bipolar nature of the target voltage. At the end of each pulse-off period the target voltage is reversed. At that instant, ions in the vicinity of the target will be accelerated by the normal negative sputtering voltage, plus the positive pulse-off voltage. Thus, at the beginning of each pulse-on period there will be a flux of ions incident at the target with a higher than average energy. Such a flux would preferentially sputter clean poisoned regions of the

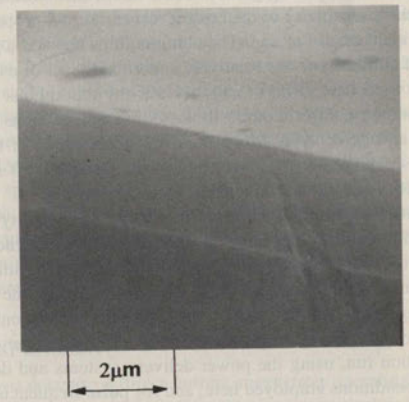

FIG. 12. SEM micrograph of an alumina film deposited onto a glass substrate at 80 kHz pulse frequency and 84% duty.

target. Since the sputtering rate from a metallic target is higher than the rate from a poisoned target, this would have the effect of raising the deposition rate. Clearly, the effectiveness of the target cleaning would be increased as the magnitude of the reverse voltage is increased, giving rise to the trend observed here. Further studies, including the use of a time-resolved Langmuir probe, are planned to investigate this in more detail.

Both arrays have demonstrated the very strong dependence of hard arc events on the duty factor selected. It appears, therefore, that it would be more appropriate to consider a critical duty factor for arc-free operation, rather than a critical frequency (accepting, again, the limited range of frequencies tested). From these experiments, a duty factor of 70% or lower is necessary, independent of pulse frequency, if arc suppression throughout the duration of a deposition run is the prime concern. The second array did show that limited periods of arc-free operation can be achieved at higher duty factors. This finding is in agreement with Belkind, Freilich, and Scholl,[9,10] who also obtained arc-free reactive sputtering of alumina for short time periods at duties greater than 90%. However, this study indicated that such conditions do not remain arc free and that breakdown soon occurs. Once this has happened, the incidence of arcing then increases at an exponential rate. The scatter observed in the data presented here probably reflects the difficulty in replicating target conditions at the beginning of each run. The target condition is certainly an important, but currently unquantified, factor. Finally, on this subject, and underlining the comments made about the target condition, there may also be some evidence to suggest that increasing the reverse voltage can be beneficial in reducing arcing. In a manner analogous to the influence of reverse voltage on deposition rate, the mechanism for this may again be preferential cleaning of the poisoned regions of the target at the beginning of each pulse-on period. This is somewhat speculative at this stage, and any actual effect is very much second order, compared to the duty factor.

The other surprising point to come out of this work is the apparent insensitivity of the coating structures and properties to the incidence of arcing. The alumina films showed a great deal of similarity at the relatively superficial level of examination used here. All coatings were x-ray amorphous with stoichiometric Al_2O_3 compositions. All structures were fully dense and defect free. More sophisticated analysis of these films is planned for the future, including nanohardness measurements and surface roughness measurements.

To summarize the findings of this work, high-quality alumina films can be deposited by pulsed reactive magnetron sputtering over a broad range of conditions. No significant differences in performance were observed between the two dc magnetron drivers used. The optimum conditions to achieve hard arc-free operation throughout the course of a deposition run, using the power delivery systems and deposition conditions employed here, and for pulse frequencies in the range 20–100 kHz, are to select a duty factor of 70%, with the reverse voltage set to 20%.

V. CONCLUSIONS

High-quality defect-free alumina films have been deposited by pulsed reactive magnetron sputtering over a broad range of conditions. A systematic study of the deposition conditions demonstrated that the incidence of hard arcs is largely controlled by the duty factor selected, and is independent of pulse frequency (over the range tested). It is more appropriate, therefore, to consider the concept of a critical duty factor for arc-free operation, rather than a critical frequency. This study indicates that for the deposition of alumina films a duty factor of 70% or lower is necessary for medium-term (i.e., several hours) arc-free operation. The deposition rate also appeared to be independent of pulse frequency, but to increase with reverse voltage at any given duty factor.

[1]M. Scherer, J. Schmitt, R. Latz, and M. Schanz, J. Vac. Sci. Technol. A **10**, 1772 (1992).
[2]P. Frach, U. Heisig, C. Gottfried, and H. Walde, Surf. Coat. Technol. **59**, 177 (1993).
[3]S. Schiller, K. Goedicke, J. Reschke, V. Kirkhoff, S. Schneider, and F. Milde, Surf. Coat. Technol. **61**, 331 (1993).
[4]D. A. Glocker, J. Vac. Sci. Technol. A **11**, 2989 (1993).
[5]B. Stauder, F. Perry, and C. Frantz, Surf. Coat. Technol. **74-75**, 320 (1995).
[6]W. D. Sproul, M. E. Graham, M. S. Wong, S. Lopez, D. Li, and R. A. Scholl, J. Vac. Sci. Technol. A **13**, 1188 (1995).
[7]P. J. Kelly, O. A. Abu-Zeid, R. D. Arnell, and J. Tong, Surf. Coat. Technol. **86-87**, 28 (1996).
[8]P. J. Kelly and R. D. Arnell, J. Vac. Sci. Technol. A **17**, 945 (1999).
[9]A. Belkind, A. Freilich, and R. A. Scholl, Surf. Coat. Technol. **108-109**, 558 (1998).
[10]A. Belkind, A. Freilich, and R. A. Scholl, J. Vac. Sci. Technol. A **17**, 1934 (1999).
[11]W. D. Sproul, Vacuum **51**, 641 (1998).
[12]J. C. Sellers, Surf. Coat. Technol. **98**, 1245 (1998).
[13]P. J. Kelly and R. D. Arnell, Vacuum **56**, 159 (2000).
[14]G. Roche and L. Mahoney, Vacuum Solutions **12**, 11 (1999).
[15]M. S. Wong, W. J. Chia, P. Yashar, J. M. Schneider, W. D. Sproul, and S. A. Barnett, Surf. Coat. Technol. **86-87**, 381 (1996).
[16]K. Koski, J. Holsa, and P. Juliet, Surf. Coat. Technol. **116-119**, 716 (1999).
[17]K. Koski, J. Holsa, and P. Juliet, Surf. Coat. Technol. **120-121**, 303 (1999).
[18]G. Brauer, J. Szczyrbowski, G. Teschner, Surf. Coat. Technol. **94-95**, 658 (1997).
[19]G. Brauer, M. Ruske, J. Szczyrbowski, G. Teschner, and A. Zmelty, Vacuum **51**, 655 (1998).
[20]J. M. Schneider and W. D. Sproul, in *Handbook of Thin Film Process Technology: 98/1 Reactive Sputtering*, edited by W. D. Westwood (IOP, Bristol, 1998).
[21]D. Carter, G. McDonough, L. Mahoney, G. A. Roche, and H. Walde, AVS 46th International Symposium, Seattle, Washington, 25–29 October (1999) (unpublished).
[22]P. J. Kelly, P. S. Henderson, R. D. Arnell, G. A. Roche, and D. Carter, AVS 46th International Symposium, Seattle, Washington, 25–29 October (1999) (unpublished).
[23]R. Roy, *A Primer on the Taguchi Method* (Van Nostrand Reinhold, New York, 1990).

Appendix 1059-B

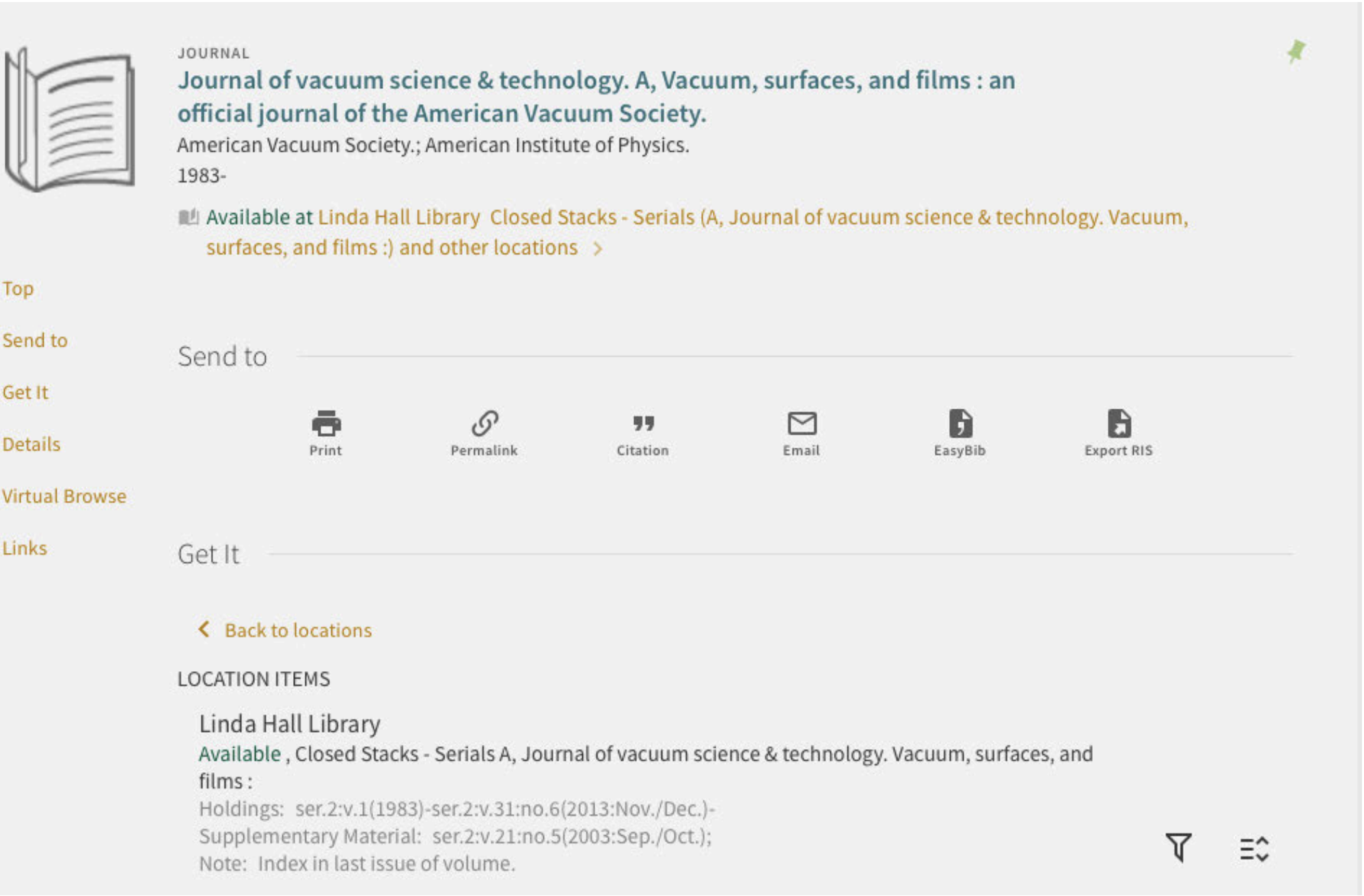
JOURNAL
Journal of vacuum science & technology. A, Vacuum, surfaces, and films : an official journal of the American Vacuum Society.
American Vacuum Society.; American Institute of Physics.
1983-
Available at Linda Hall Library Closed Stacks - Serials (A, Journal of vacuum science & technology. Vacuum, surfaces, and films :) and other locations
Top
Send to
Get It
Details
Virtual Browse
Links
Send to
Print
Permalink
Citation
Email
EasyBib
Export RIS
Get It
Back to locations
LOCATION ITEMS
Linda Hall Library
Available , Closed Stacks - Serials A, Journal of vacuum science & technology. Vacuum, surfaces, and films :
Holdings: ser.2:v.1(1983)-ser.2:v.31:no.6(2013:Nov./Dec.)-
Supplementary Material: ser.2:v.21:no.5(2003:Sep./Oct.);
Note: Index in last issue of volume.

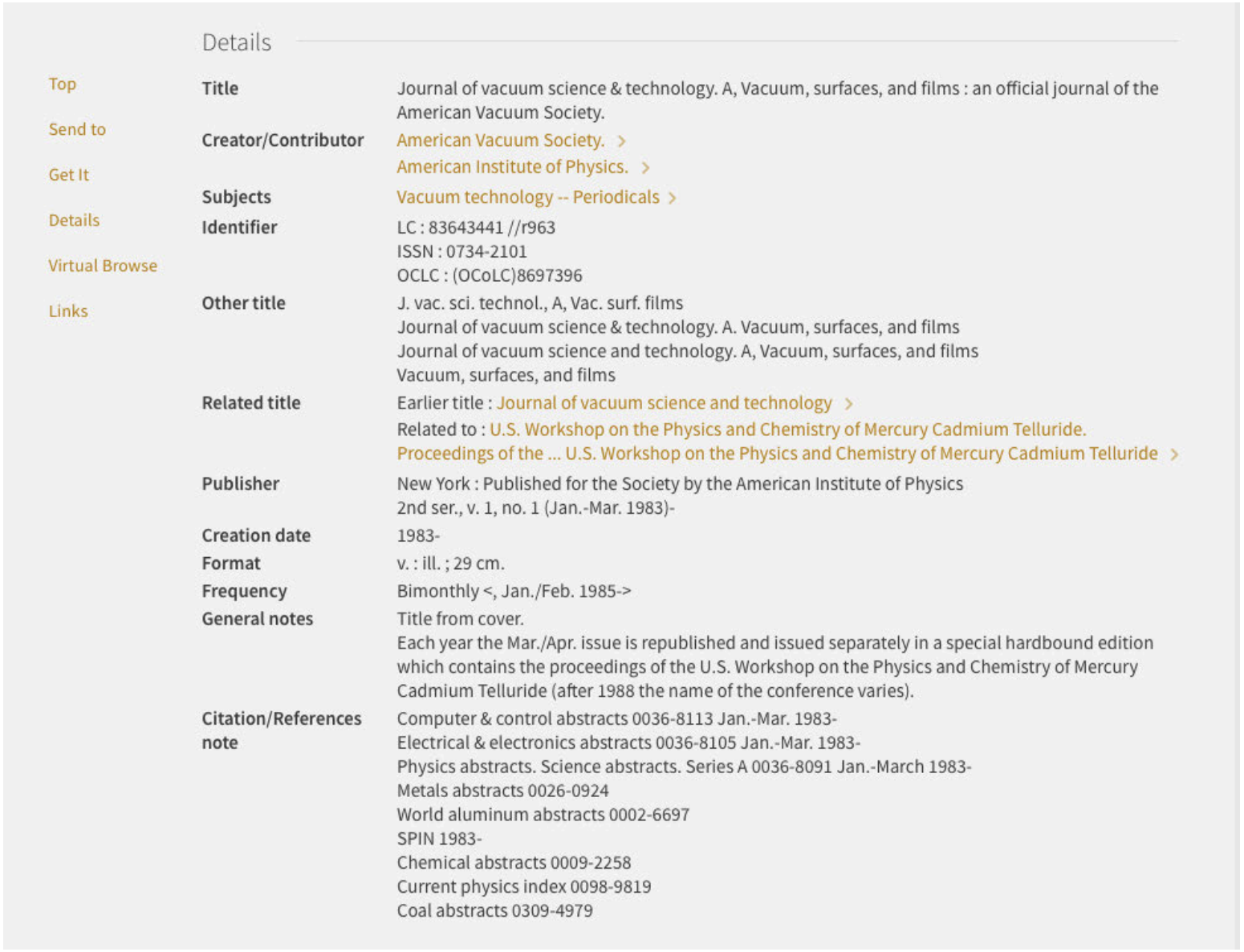

Top
Send to
Get It
Details
Virtual Browse
Links

Details

Title	Journal of vacuum science & technology. A, Vacuum, surfaces, and films : an official journal of the American Vacuum Society.
Creator/Contributor	American Vacuum Society. › American Institute of Physics. ›
Subjects	Vacuum technology -- Periodicals ›
Identifier	LC : 83643441 //r963 ISSN : 0734-2101 OCLC : (OCoLC)8697396
Other title	J. vac. sci. technol., A, Vac. surf. films Journal of vacuum science & technology. A. Vacuum, surfaces, and films Journal of vacuum science and technology. A, Vacuum, surfaces, and films Vacuum, surfaces, and films
Related title	Earlier title : Journal of vacuum science and technology › Related to : U.S. Workshop on the Physics and Chemistry of Mercury Cadmium Telluride. Proceedings of the ... U.S. Workshop on the Physics and Chemistry of Mercury Cadmium Telluride ›
Publisher	New York : Published for the Society by the American Institute of Physics 2nd ser., v. 1, no. 1 (Jan.-Mar. 1983)-
Creation date	1983-
Format	v. : ill. ; 29 cm.
Frequency	Bimonthly <, Jan./Feb. 1985->
General notes	Title from cover. Each year the Mar./Apr. issue is republished and issued separately in a special hardbound edition which contains the proceedings of the U.S. Workshop on the Physics and Chemistry of Mercury Cadmium Telluride (after 1988 the name of the conference varies).
Citation/References note	Computer & control abstracts 0036-8113 Jan.-Mar. 1983- Electrical & electronics abstracts 0036-8105 Jan.-Mar. 1983- Physics abstracts. Science abstracts. Series A 0036-8091 Jan.-March 1983- Metals abstracts 0026-0924 World aluminum abstracts 0002-6697 SPIN 1983- Chemical abstracts 0009-2258 Current physics index 0098-9819 Coal abstracts 0309-4979

```
03665cas a2200613 a 4500
992759783405961
20191030185458.0
820818c19839999nyubr1p       0   a0eng d
##$a   83643441 //r963 $zsn 82003445
##$a3 $b3 $i8403 $j2 $k1 $l1 $m1
0#$a0734-2101
##$aJVTAD6
##$a716990 $bUSPS
##$a(OCoLC)8697396
##$9382241
##$a(MoKL)275978-lhalldb
##$a(lhalldb)275978-lhalldb
##$bAIP Subscription Fulfillment Division, 500 Sunnyside Blvd., Woodbury, NY 11797
##$aNSD $cNSD $dHUL $dNST $dDLC $dNST $dSER $dNST $dDLC $dAIP $dNST $dAIP $dNSD $dNST $dNSD $dAIP $dDLC $dNST $dNSD $dDLC $dWAU $dLHL
##$ansdp $alc
##$aLHLA
00$aTJ940 $b.J668
0#$aJ. vac. sci. technol., A, Vac. surf. films
#0$aJournal of vacuum science & technology. A. Vacuum, surfaces, and films
00$aJournal of vacuum science & technology. $nA, $pVacuum, surfaces, and films : $ban official journal of the American Vacuum Society.
10$aJournal of vacuum science and technology. $nA, $pVacuum, surfaces, and films
10$aVacuum, surfaces, and films
##$aNew York : $bPublished for the Society by the American Institute of Physics, $c1983-
##$av. : $bill. ; $c29 cm.
##$aBimonthly $b<, Jan./Feb. 1985->
##$aQuarterly, $bJan.-Mar. 1983-
0#$a2nd ser., v. 1, no. 1 (Jan.-Mar. 1983)-
##$aTitle from cover.
1#$aComputer & control abstracts $x0036-8113 $bJan.-Mar. 1983-
1#$aElectrical & electronics abstracts $x0036-8105 $bJan.-Mar. 1983-
1#$aPhysics abstracts. Science abstracts. Series A $x0036-8091 $bJan.-March 1983-
2#$aMetals abstracts $x0026-0924
2#$aWorld aluminum abstracts $x0002-6697
1#$aSPIN $b1983-
2#$aChemical abstracts $x0009-2258
2#$aCurrent physics index $x0098-9819
2#$aCoal abstracts $x0309-4979
##$a2nd series, vol.21, no.5 includes a separate supplement titled: 50 Years of science, technology, and the AVS (1953-2003)
```

```
##$a2nd series, vol.21, no.5 includes a separate supplement titled: 50 Years of science, technology, and the AVS (1953-2003)
##$aIssued also on microfilm.
##$aEach year the Mar./Apr. issue is republished and issued separately in a special hardbound edition which contains the proceedings of the U.S. Wo
#0$aVacuum technology $vPeriodicals.
2#$aAmerican Vacuum Society.
2#$aAmerican Institute of Physics.
01$tJournal of vacuum science and technology $x0022-5355 $w(OCoLC)1754855 $w(DLC) 68053979
1#$aU.S. Workshop on the Physics and Chemistry of Mercury Cadmium Telluride. $tProceedings of the ... U.S. Workshop on the Physics and Chemistry of
##$aAAP $aArU $aAzU $aCLSU $aCSt $aCU $aCU-A $aCU-I $aCU-RivP $aCU-S $aCU-SB $aCaAEU $aCaNSHD $aCaOLU $aCaOOM $aCaOTCL $aCaOTU $aCaOWA $aCaOWtU $aC
##$aJournal of vacuum science & technoglogy. A, Vacuum, surfaces, and films.
##$cSer
##$aJan./Feb. 1985
##$bJournal of vacuum science & technology. A, Vacuum, surfaces, and films : an official journal of the American Vacuum Society.
##$aLTI 04/26/2017
```